A COMPARISON OF VARIOUS COHERENT OPTICAL FILTERING OPERATIONS

Robert Lee Cody

ARO, Inc.

June 1971

TECHNICAL REPORTS
FILE COPY

ARNOLD ENGINEERING DEVELOPMENT CENTER
AIR FORCE SYSTEMS COMMAND
ARNOLD AIR FORCE STATION, TENNESSEE

NOTICES

A COMPARISON OF VARIOUS COHERENT
OPTICAL FILTERING OPERATIONS

Robert Lee Cody
ARO, Inc.

FOREWORD

The research reported herein was sponsored by Arnold Engineering Development Center (AEDC), Air Force Systems Command (AFSC), Arnold Air Force Station, Tennessee, under Program Element 64719F.

The results of the research presented were obtained by ARO, Inc. (a subsidiary of Sverdrup & Parcel and Associates, Inc.), contract operator of the AEDC, AFSC, Arnold Air Force ·Station, Tennessee, under Contract F40600-71-C-0002. The investigation was conducted under ARO Project No. BC5116, and the manuscript was submitted for publication on May 11, 1971.

The author wishes to express his sincere appreciation to Dr. J. D. Trolinger of ARO, Inc., for his invaluable help and advice throughout the study. Appreciation is expressed to Dr. T. H. Gee for his valuable comments and suggestions. This report describes work performed by the author while working for Experimental Research, Technical Staff, ARO, Inc., as a graduate assistant and attending the University of Tennessee Space Institute under the support of the Air Force Institute of Technology. The material reported herein was submitted to the University of Tennessee as partial fullfilment of the requirements of the degree of Master of Science.

This technical report has been reviewed and is approved.

David C. Francis
Captain, USAF
Research and Development
    Division
Directorate of Technology

Harry L. Maynard
Colonel, USAF
Director of Technology

ABSTRACT

A comparison is made of different coherent optical filters with respect to their ability to locate an edge and identify phase information. These different filtering methods are bandpass filtering, the Schlieren method, the Hilbert transform method, a linear amplitude filter, and a differential filter; these filters are one-dimensional. The differential filter is a combination of two filters, a linear amplitude filter and a Hilbert transform filter. A linear amplitude filter is made photographically by a programmed exposure of film to give the correct density variations. A Hilbert transform filter is a phase filter which is accomplished with a dielectric coating on glass. Bandpass filtering is accomplished by using a wire. With the use of a razor blade, the Schlieren method is achieved. The comparison of these filters indicates that bandpass filtering is superior for the location of an edge and that the Hilbert transform method is best for identifying phase information.

TABLE OF CONTENTS

LIST OF FIGURES

FIGURE   PAGE

NOMENCLATURE

a	Lower cutoff frequency of the bandpass filter
A_{max}	Maximum value of the filter $A'(\omega)$
A_{min}	Minimum value of the filter $A'(\omega)$
$A(\omega)$	Linear amplitude filter
$A'(\omega)$	Approximate linear amplitude filter
b	Upper cutoff frequency of the bandpass filter
B	Lower cutoff frequency of the filter $A'(\omega)$
B_m	Lower magnification cutoff frequency of the filter $A'(\omega)$
B_r	Lower radial cutoff frequency of the filter $A'(\omega)$
c	Velocity of a light wave in a vacuum
cm	Centimeters (10^{-2} meters)
d	Half of the width of the filter $A'(\omega)$
D	Film density
d_n	Normal thickness
$d_{\pi/4}$	Thickness at an angle of 45°
e	Base of the natural logarithm
E	Exposure
E_o	Exposure for the density equal to zero
f	Focal length of a lens
fcs	Foot candle · seconds
$F(\omega)$	Differential filter
$F'(\omega)$	Approximate differential filter
$\mathfrak{F}$	Indicates Fourier transform

$\mathcal{F}^{-1}$	Indicates inverse Fourier transform
$G(\omega_x, \omega_y)$	Fourier transform of $g(x,y)$
$G(x)$	Amplitude of edge due to bandpass filtering
$g(x,y)$	General variable
$H(\omega)$	Hilbert transform filter
I	Intensity
$I_i(x_i)$	Intensity in the image plane
I_o	Constant intensity
j	$\sqrt{-1}$
k	Slope of the filter $A'(\omega)$
k'	Slope of the filter $A'(x_f)$
k_1	Slope of the linear portion of the amplitude transmission versus exposure curve
k_r	Slope of the filter $F'(\omega_r)$
L	Lens
m	Magnification
mm	Millimeters (10^{-3} meters)
mv	Millivolts (10^{-3} volts)
MHz	Megahertz (10^{6} hertz)
n	Index of refraction
n_a	Index of refraction of air
n_b	Index of refraction of a dielectric material
$nsec$	Nanoseconds (10^{-9} seconds)
q	Image distance from lens
RPM	Speed of the D. C. motor with units rpm
rpm	Revolution per minute

$s(x_o)$	Amplitude transmission of the step function
Si	Sine integral
t	Time
t'	Time required for a light wave to travel through a certain dielectric material thickness
T_A	Amplitude transmission
T_o	Amplitude transmission for the exposure equal to zero
$T(\omega)$	Filter for the Schlieren method
$U(x_i)$	Amplitude in the image plane
$U(\omega)$	Amplitude in the frequency plane
v	Velocity of the edge
v_1	Slope of the function x_{f1}
v_2	Slope of the function x_{f2}
v_o	The value at which the slope of x_{f1} and x_{f2} are equal
vdc	D. C. volts
V_{DC}	The D. C. voltage input to the motor
W	Upper cutoff frequency of the filter $A'(\omega)$
W_m	Upper magnification cutoff frequency of the filter $A'(\omega)$
W_r	Upper radial cutoff frequency of the filter $A'(\omega)$
x_f	Distance in the frequency plane
x_{f1}	Distance variable for the portion of the filter $A'(x_f)$ described by the H and D curve

x_{f2} — Distance variable for the portion of the filter $A'(x_f)$ described by the amplitude transmission versus exposure curve

x_i — x-coordinate in the image plane

x_o — x-coordinate in the object plane

y_i — y-coordinate in the image plane

y_o — y-coordinate in the object plane

γ — Slope of the linear portion of the H and D curve

$\delta(\omega)$ — Delta function

ζ — Constant angle of the filter $F'(\omega)$

η — Positive integer

θ — Angle between the x axis of a filter and ω_x axis of the frequency plane

$\theta(\omega)$ — Phase filter

κ — Wave number

λ — Wavelength of light source

μsec — Microseconds (10^{-6} seconds)

ν — Velocity of a light wave in a medium

ν_a — Velocity of a light wave in air

ν_b — Velocity of a light wave in a dielectric material

τ — Width of the function $s'(x_o)$

ω — Spatial frequency

ω_r — Radial spatial frequency

ω_x — Spatial frequency along x axis of frequency plane

ω_y — Spatial frequency along y axis of frequency plane

$*$ — Convolution integral

$\wedge$ — Hilbert transform

CHAPTER I

INTRODUCTION

A major product of scientific and engineering endeavors is the data resulting from experiments and tests. In this thesis, an area of data processing which might appropriately be called data enhancement is addressed. Much of the data encountered in this work has arisen from aerodynamic simulation and testing; however, the techniques which will be discussed are not limited to problems in the field of aerodynamics.

Of primary interest here are data relating to dimensional changes and phase changes. Dimensional changes might correspond to the ablation of a projectile fired through a chamber, where the phase changes might correspond to density, temperature and pressure gradients about a subject under test. The techniques which are employed in this investigation are coherent optical spatial filtering techniques. Basic to the application of such techniques is the simplicity resulting from use of a simple positive lens to effect a two-dimensional Fourier transformation. An imaging-transform configuration is depicted by Figure 1 which may be employed for performing spatial filtering operations. Such a system utilizes the laser as its source of coherent light.

Collimated
Coherent
Light
Source

f

Object
Plane

Positive
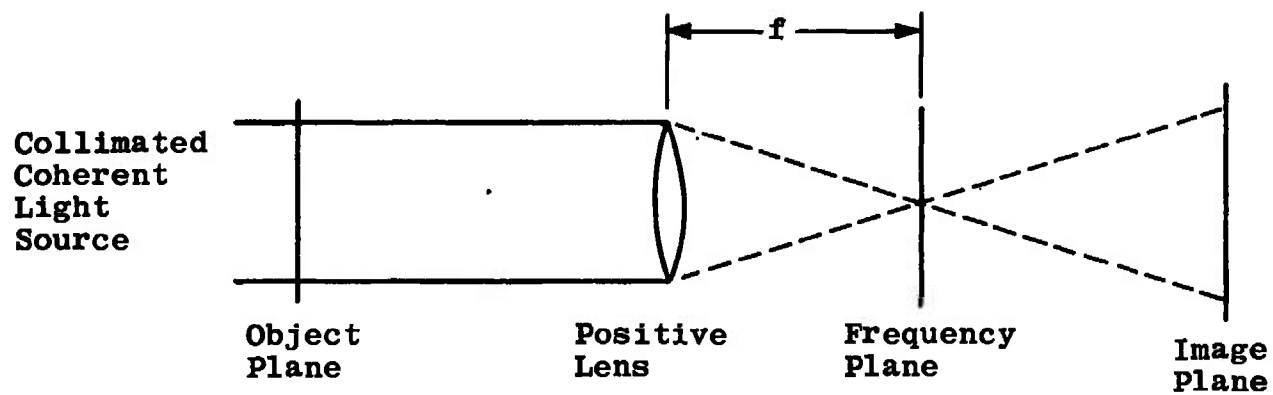Lens

Frequency
Plane

Image
Plane

Figure 1. A simple coherent optical data processing system.

As stated above, coherent optical data processing is based on the Fourier transform. The Fourier transform is defined as

$$\mathcal{F}\{g(x,y)\} =$$

$$\int_{-\infty}^{\infty} \int_{-\infty}^{\infty} g(x,y) e^{-j(\omega_x x + \omega_y y)} \, dxdy = G(\omega_x, \omega_y) \qquad (1)$$

and the inverse Fourier transform is

$$\mathcal{F}^{-1}\{G(\omega_x, \omega_y)\} =$$

$$\frac{1}{4\pi^2} \int_{-\infty}^{\infty} \int_{-\infty}^{\infty} G(\omega_x, \omega_y) e^{+j(\omega_x x + \omega_y y)} \, d\omega_x d\omega_y \qquad (2)$$

A positive lens will perform the Fourier transform of an input in the object plane of the lens. The transform is located in the focal plane or generally referred to as the frequency plane. The frequency, ω, is a spatial frequency of units lines/mm. The image plane of the lens is the Fourier transform of the frequency plane, or

$$\mathcal{F}\{\mathcal{F}\{g(x_o, y_o)\}\} = g(x_i, y_i) = g(-x_o, -y_o) \qquad (3)$$

where (x_i, y_i) are the coordinates of the image plane, and

3

(x_o, y_o) are the coordinates of the object plane. Both coordinate units are usually millimeters. Generally, the processing of data in the object plane is accomplished by filtering in the frequency plane, and the result is observed in the image plane [1].[1]

In the past, a variety of different means has been used to process optical information that is not visible to the unaided eye, and to minimize the error in the location of an edge of an object. Some of the common methods previously used are bandpass filtering, the Schlieren method, the Hilbert transform method, and the differential filtering method.

The Schlieren method is effected by blocking half of the frequencies in the frequency plane with a razor blade, for example. The Schlieren method may be described as a filtering process, the filter being expressed as [1]

$$T(\omega) = \frac{1}{2}(1 + \text{sgn}(\omega)) \qquad (4)$$

where the function $\text{sgn}(\omega)$ is defined as

$$\text{sgn}(\omega) = \begin{bmatrix} -1 & \omega < 0 \\ 0 & \omega = 0 \\ 1 & \omega > 0 \end{bmatrix} \qquad (5)$$

---

[1]Numbers in brackets correspond to similarly numbered references in the bibliography.

The Schlieren method is used in both accentuating an edge of an input and in the conversion of phase information to intensity information.

The Hilbert transform method consists of applying to the negative frequencies a phase shift of $+ \pi/2$ radians and to the positive frequencies a phase shift of $- \pi/2$ radians. The Hilbert transform filter is described by [2]

$$H(\omega) = -j \ \text{sgn}(\omega) \tag{6}$$

where $j^2 = -1$. This filter is fabricated by coating one-half of a glass plate with a dielectric material to give a phase shift of π radians. The thickness of the dielectric material retards the light wave by $\lambda/2$. The Hilbert transform is used to convert phase information to intensity information [3].

A bandpass filter is the sum of a high pass filter and a low pass filter. The high pass filter is realized by placing an opaque disc at the center of the frequency plane for a two-dimensional input or a wire at the center of the frequency plane for the one-dimensional input. The low pass filter may also be realized by limiting the aperture to cut off the higher frequencies. In practice, the low pass filter may result from the lens used to perform the Fourier transform of the input in the object plane. The bandpass filter is used to accentuate the edge of an input.

5

The differential filter is a complex linear amplitude filter of

$$F(\omega) = j\omega$$

$$= |\omega| \; j \; \text{sgn}(\omega) \tag{7}$$

The differential filter is composed of two filters, a linear amplitude filter and a phase filter. This theoretical filter cannot be realized because it is physically impossible to have $F(\omega) = 0$ at $\omega = 0$ [4]. However, an approximate one-dimensional differential filter can be fabricated. The reasons for the approximation and the limitations that they impose are discussed in Chapter II. Both phase information and edges of an input are accentuated by the differential filter.

Use of a differential filter was suggested by Eguchi and Carlson [5]. Other authors have stated that they used a differential filter in optical correlation systems to improve the signal-to-noise ratio, but no mention was made of the approximation made to represent a differential filter [6,7]. Some authors have synthesized optical information and a differential filter on the computer [8,9].

The apparatus and the methods used in developing the linear amplitude filter and phase filter are discussed in Chapter II. Chapter III gives an experimental comparison of the various optical filtering methods operating on a

one-dimensional step function and phase information.
Comparative conclusions relevant to the advantages of the
various filters are made in Chapter IV.

CHAPTER II

THE OPTICAL DIFFERENTIAL FILTER

I.   THE THEORY OF THE DIFFERENTIAL FILTER

Consider the one-dimensional case of an input, g(x), in the object plane of the lens in Figure 1, page 2. The Fourier transform of g(x) is $G(\omega)$. To find the type of filter needed to perform the derivative of the input, g(x), the Fourier transform of the derivative must be known. The Fourier transform of dg/dx is [2]

$$\frac{dg(x_o)}{dx_o} = \frac{d}{dx_o} [\mathcal{F}^{-1} \{G(\omega)\}]$$

$$= \frac{1}{2\pi} \frac{d}{dx_o} [\int_{-\infty}^{\infty} G(\omega) e^{j\omega x_o} d\omega]$$

$$= \frac{1}{2\pi} \int_{-\infty}^{\infty} j\omega G(\omega) e^{j\omega x_o} d\omega \qquad (8)$$

Therefore,

$$\mathcal{F}\{\frac{dg(x_o)}{dx_o}\} = j\omega G(\omega) \qquad (9)$$

Thus, in order to differentiate the input, a filter of complex amplitude transmittance, $j\omega$, is placed in the

frequency plane. Then the function in the image plane is $dg(-x_o)/dx$.

The ideal differential filter, $F(\omega)$, is composed of two filters, a linear amplitude filter, $A(\omega)$, and a phase filter, $\theta(\omega)$, which are shown in Figure 2. Since the difference between the negative and positive frequencies is π radians for the phase filter, it is fabricated as a filter that shifts half the frequency plane by π radians [5]. The linear amplitude filter is made using film, but there is a discontinuity at the origin since the film will not record infinite densities [4]. The amplitude transmission of the film is limited to the values A_{max}, which is less than unity, and A_{min}, which is greater than zero. The amplitude transmission limits of the film make the linear amplitude filter bandpass limited. The phase filter is also bandpass limited. Therefore, an approximation is made of the differential filter; it is the filter $F'(\omega)$ as shown in Figure 3 [5]. The function rect $(\omega/2B)$ is a high pass filter. Its purpose is to eliminate the low spatial frequencies, $(0 \leq |\omega| \leq B)$. The amplitude transmission value of A_{min} occurs at the spatial frequencies $\pm B$, and the value A_{max} occurs at the frequencies $\pm W$. The linear amplitude filter has a slope, k, which is generally less than one.

When the input $g(x_o)$ is filtered by the approximate differential filter, the amplitude, $U(\omega)$, in the frequency plane is
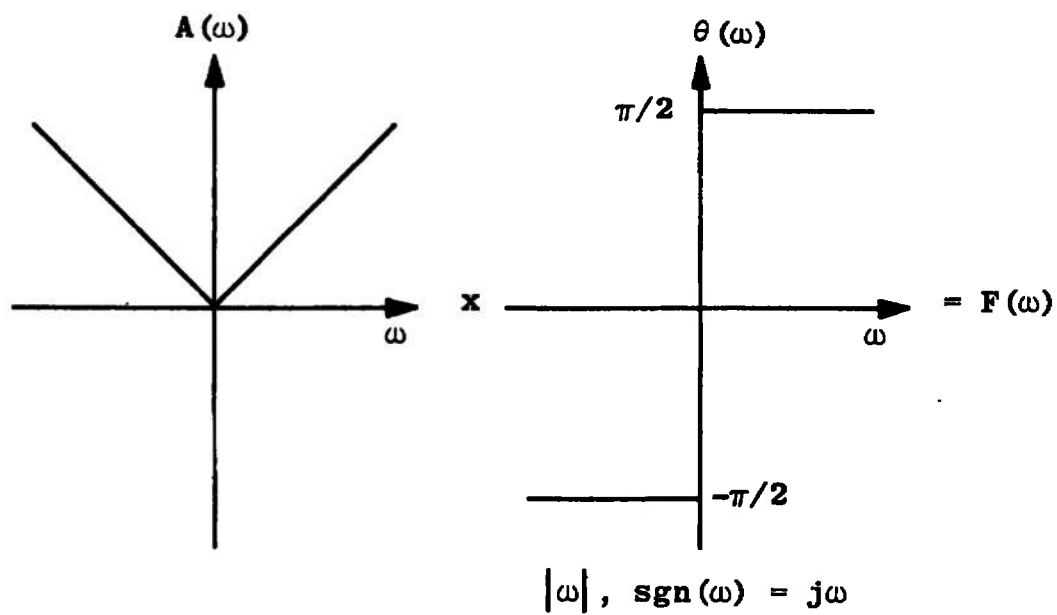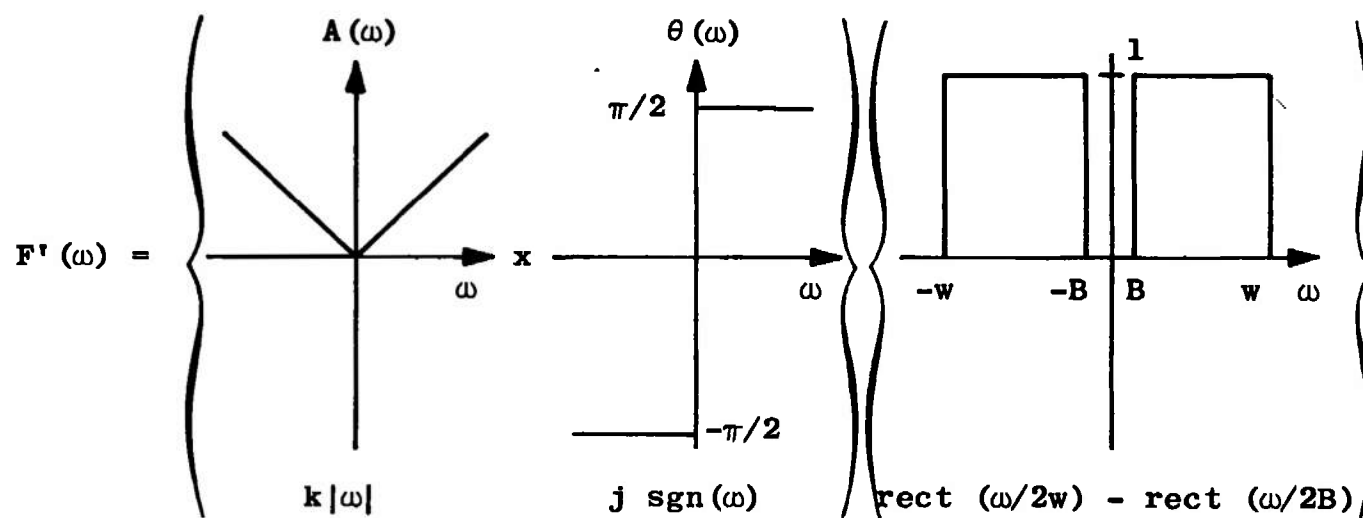
Figure 2.   The differential filter.

$$F'(\omega) = \begin{cases} & \end{cases}$$

A(ω)

ω

k$|\omega|$

θ(ω)

$\pi/2$

x

ω

$-\pi/2$

j sgn(ω)

1

$-$w $-$B   B   w ω

rect ($\omega/2$w) $-$ rect ($\omega/2$B)

Figure 3.   The approximate differential filter.

$$U(\omega) = G(\omega)F'(\omega)$$

$$= jk\omega\, G(\omega)\, [\text{rect}\, [\frac{\omega - \frac{W-B}{2}}{W-B}] + \text{rect}\, [\frac{\omega + \frac{W+B}{2}}{W-B}]] \quad (10)$$

and the amplitude in the image plane is

$$U(x_i) = \mathfrak{F}\{G(\omega)F'(\omega)\}$$

$$= \mathfrak{F}\{jk\omega\, G(\omega)\} * \mathfrak{F}\{\text{rect}\, [\frac{\omega - \frac{W-B}{2}}{W-B}]\}$$

$$+ \mathfrak{F}\{jk\omega\, G(\omega)\} * \mathfrak{F}\{\text{rect}\, [\frac{\omega + \frac{W+B}{2}}{W-B}]\} \quad (11)$$

$$= k\, \frac{dg(x_i)}{dx_i} * (W-B)\, \text{sinc}\, [(W-B)x_i]e^{-j(\frac{W+B}{2})x_i}$$

$$+ k\, \frac{dg(x_i)}{dx_i}\, (W-B)\, \text{sinc}\, [(W-B)x_i]e^{+j(\frac{W+B}{2})x_i} \quad (12)$$

$$= 2(W-B)k\, \frac{dg(x_i)}{dx_i} * \text{sinc}\, [(W-B)x_i]\cos[(\frac{W+B}{2})x_i] \quad (13)$$

The symbol * denotes the convolution integral. This is the image amplitude of the input $g(x_o)$ filtered by the approximate differential filter $F'(\omega)$ in a single lens system such as Figure 1, page 2.

The slope and the bandwidth of the filter $F'(\omega)$ is changed by the magnification of the frequency plane. The

slope of the filter $F'(\omega)$ is related to the magnification, m, as

$$F'(\omega) = jmk\omega \tag{14}$$

and the cutoff frequencies as

$$W_m = \frac{W}{m} \tag{15}$$

$$B_m = \frac{B}{m} \tag{16}$$

The approximate one-dimensional differential filter has a complex linear amplitude transmission along the x axis and constant amplitude transmission along different points on the y axis. The y axis is bandlimited by the function rect (ω_y/W_y) just as the x axis is bandlimited by the function rect (ω_x/W_x). This does not affect the derivative of a one-dimensional input, but it does affect a two-dimensional input. As the filter $F'(\omega)$ is rotated in the frequency plane, the slope is decreased and the bandwidth changes. The filter $F'(\omega)$ in terms of polar coordinates becomes

$$F'(\omega_r) = jk_r\omega_r \tag{17}$$

where

$$k_r = k \cos\theta \tag{18}$$

and ω_r is the spatial frequency with respect to the radius. For $\theta - 0°$

$$F'(\omega_r) = F'(\omega_x) \tag{19}$$

The filter $F'(\omega_r)$ will equal zero at the angle

$$\theta = \tan^{-1} \left(\frac{W_y}{B_x}\right) \tag{20}$$

With the rotation of the filter, the upper cutoff frequency is

$$W_r = (W_x^2 + W_y^2)^{1/2} \cos(\theta - \zeta) \tag{21}$$

where

$$\zeta = \tan^{-1} \left(\frac{W_y}{W_x}\right) \tag{22}$$

The lower cutoff frequency is

$$B_r = B \sec \theta \tag{23}$$

Higher order derivatives are generated as long as a filter $(j\omega)^\eta$ is realized. The ηth order derivative is [5]

$$\frac{d^\eta g(x)}{dx} = \mathcal{F}^{-1} \{(j\omega)^\eta \, G(\omega)\}$$

II. FABRICATION OF THE DIFFERENTIAL FILTER

The Linear Amplitude Filter

The differential filter is composed of two filters, a linear amplitude filter, $A(\omega)$, and a phase filter, $\theta(\omega)$. The linear amplitude filter is approximated by the filter $A'(\omega)$ as shown in Figure 4. The filter $A'(\omega)$ is obtained on film by varying the exposure to the film. Since a one-dimensional amplitude filter is required, the exposure is varied one-dimensionally by an edge of a plate moving across a uniform light source at a programmed rate.

The filter $A'(\omega)$ is related to distance by

$$\omega = \frac{x_f}{\lambda f} \tag{25}$$

where x_f is a distance in the frequency plane, λ is the wavelength of the coherent light source, and f is the focal length of a lens [1].

The filter $A'(\omega)$ is a distance 2d in width, and d is defined as

$$d = \lambda f W \tag{26}$$

Since the filter $A'(\omega)$ is an even function, the exposure is varied identically for the distances $\pm$ d. The amplitude of the filter $A'(\omega)$ is the amplitude transmission of the film, T_A , which is a function of exposure. Hence, for the correct variations of the exposure, the distance must be
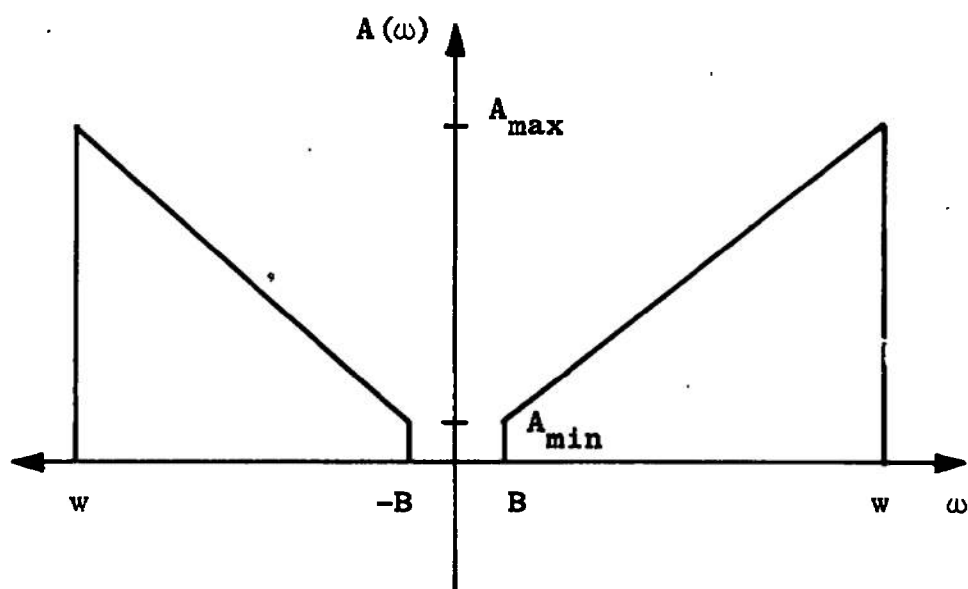
Figure 4. The linear amplitude filter $A'(\omega)$.

expressed as a function of exposure to give the correct amplitude transmission for the filter. The velocity of the edge determines the rate-of-change of the exposure, and this is derived from the derivative of the distance-exposure equation.

The correct exposure control. The amplitude transmission of the film is a function of the film density, D, and it is defined as [1]

$$T_A = 10^{-D/2} \qquad (27)$$

The density of the film is a function of the exposure. The relationship of the exposure and film density is best expressed linearly with the well-known Hurter-Driffield curve, but this curve usually is not linear for densities less than 0.8. Therefore, the amplitude transmission versus exposure curve is used to give a linear relationship of the exposure and amplitude transmission for densities less than 0.8. This curve is linear for the non-linear portion of the H and D curve. Each of these curves are shown in Figure 5 for a typical film.

For the H and D curve, the film density is [1]

$$D = \gamma \log \left(\frac{E}{E_o}\right) \qquad (28)$$

where γ is the slope of linear portion, E is the exposure,
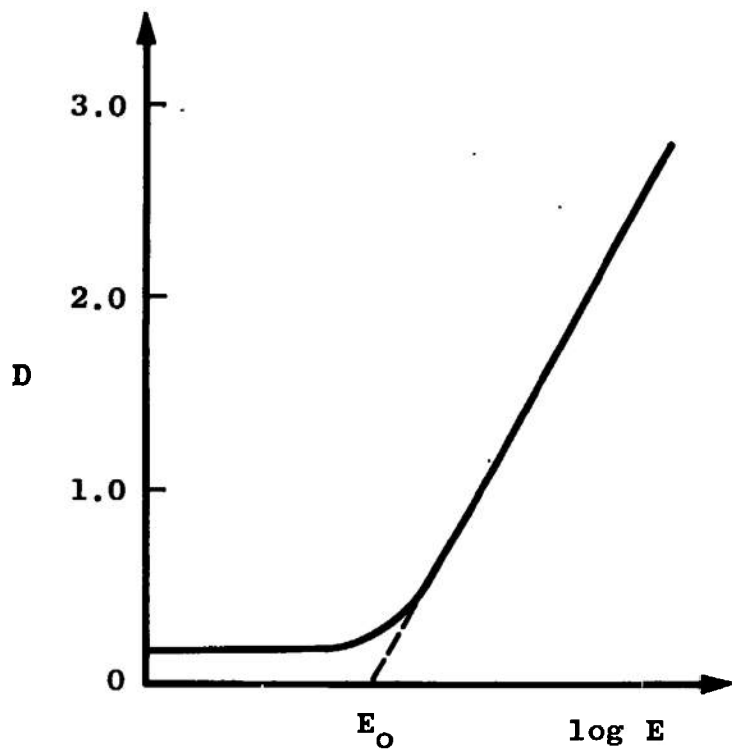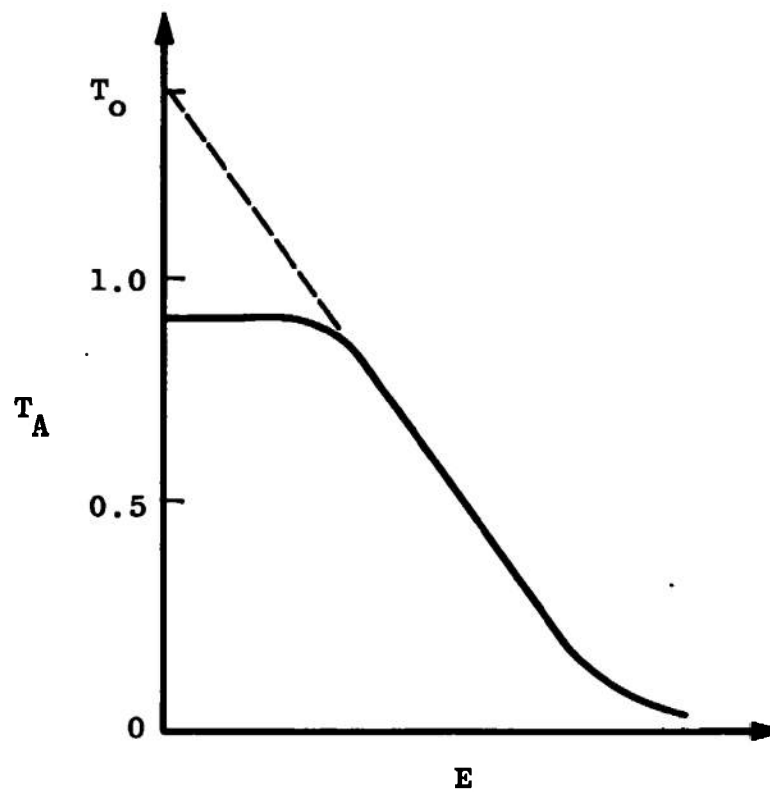
(a) H and D curve

(b) Amplitude transmission versus exposure curve

Figure 5. Film characteristic curves.

and E_O is the value of the exposure for the density equal to zero. The log is to the base ten.

From Equations (27) and (28), the amplitude transmission of the film is

$$T_A(E) = (\frac{E_O}{E})^{\gamma/2} \tag{29}$$

The amplitude transmission versus exposure curve is described as [10]

$$T_A(E) = T_O - k_1 E \tag{30}$$

where T_O is the amplitude transmission for the exposure equal to zero, and k_1 is the slope of the linear portion.

For the bandpass section of the amplitude filter,

$$A'(\omega) = k|\omega| \tag{31}$$

or as a function of distance in the frequency plane

$$A'(x_f) = k'|x_f| \tag{32}$$

where $k' = k/\lambda f$. Since the filter $A'(\omega)$ is made photographically,

$$T_A(x_f) = k'|x_f| \tag{33}$$

From Equation (29)

$$k' |x_f| = (\frac{E_o}{E})^{\gamma/2} \tag{34}$$

for the linear portion of the H and D curve, and from
Equation (30)

$$k' |x_f| = T_o - k_1 E \tag{35}$$

for the linear portion of the amplitude versus exposure
curve.

Both expressions for the distance, x_f , are
dependent on the variable E, the exposure. The exposure is
defined as intensity, I, times time, t(1), or

$$E = It \tag{36}$$

This gives two independent variables. From observation, it
is readily noticeable that a single independent variable is
much easier to handle, and since time is easier to vary, the
intensity is held constant. Then Equation (34) becomes

$$|x_{f1}| = \frac{1}{k'} (\frac{E_o}{I_o})^{\gamma/2} t^{-\gamma/2} \tag{37}$$

and Equation (35) becomes

$$|x_{f2}| = \frac{T_o}{k'} - \frac{k_1}{k'} I_o t \tag{38}$$

where I_o is a constant intensity and the section of the filter $A'(\omega)$ based on the H and D curve is denoted by x_{f1} and x_{f2} denotes the section based on the amplitude transmission versus exposure curve.

The velocity that the edges must travel across the uniform light source to give the correct exposure variation is found by taking the derivative of Equations (37) and (38) with respect to time. The velocity from Equation (37) is

$$v_1 = \pm \frac{\gamma}{2K'} \left(\frac{E_o}{I_o}\right)^{\gamma/2} t^{-1/2(\gamma+2)} \tag{39}$$

and the velocity from Equation (38) is

$$v_2 = \pm \frac{k_1}{k'} I_o \tag{40}$$

The function $|x_{f1}|$ is valid for the small values of the amplitude transmission and the function $|x_{f2}|$ is valid for the larger values of the amplitude transmission.

The velocity, v_o , is where

$$v_1 = v_2 = v_o \tag{41}$$

The function, x_{f1} , is invalid for $v_1 > v_o$, and the function, x_{f2} , is invalid for $v_2 < v_o$.

Fabricating the linear amplitude filter. The method used to traverse the edges must be kept in mind when

selecting the film to be used. One of the simplest methods

is the use of a D. C. motor to move the edges. The D. C.

motor must traverse the edges at the velocities required by

Equations (39) and (40). The edges are mounted on threaded

rods with 16 threads/inch. For every 16 turns of the rod,

the edges move one inch. The threaded rods are connected to

gears which are linked with a gear mounted to the motor's

shaft. The ratio of the gears reduces the motor by 12/19.

The method for traversing the edges is discussed later in

this chapter.

The velocity of the edge is a function of γ and k_1

of the film and of the exposure time. Gamma, γ, is the

slope of the H and D curve, k_1 is the slope of the amplitude

transmission versus exposure curve, and the exposure time is

the time required to achieve a certain density. A film with

a low γ and k_1 , a high density capability, and a long

exposure time is desired. The higher γ and k_1 , the greater

the motor velocity range capability of the motor needed to

move the edges. If the film has a low γ, it also has a low

density capability, and vice versa. The shorter the

exposure time, the greater the velocity that the edges must

travel. Kodak 649-F film came the closest to these desired

requirements.

To accurately generate the filter $A'(\omega)$, the

characteristic curves of the film being used must be known.

The curves for the Kodak 649-F 4 x 5 inch plate was obtained

by exposing three density step wedges, placed against the
film, at an intensity of 5 foot candles for a period of 20
seconds and processing the film in Kodak D-19 developer for
three minutes at 76°F. The resulting H and D curve and
amplitude transmission versus exposure curve are shown in
Figure 6.

From Figure 6, the constants for Equations (39)
and (40) were calculated to give the following:

$$E_O = 10.0 \text{ foot candles/sec}$$

$$\gamma = 4.57$$

$$T_O = 1.22$$

$$k_1 = 0.0531$$

$$I_O = 3.75 \text{ foot candles}$$

The velocity v_2 is then

$$v_2 = \pm \frac{1}{5k'} \text{ cm/sec} \tag{42}$$

Since the velocity v_2 is the maximum velocity of
the edges, the slope, k', of the filter $A'(x_f)$ is selected
to have the velocity v_2 nearest the maximum capability of
the D. C. motor used to traverse the edges. The slope, k',
was selected to be 0.2. Then, the value of the v_2 and v_1 is

$$v_2 = \pm 1.0 \text{ cm/sec} \tag{43}$$
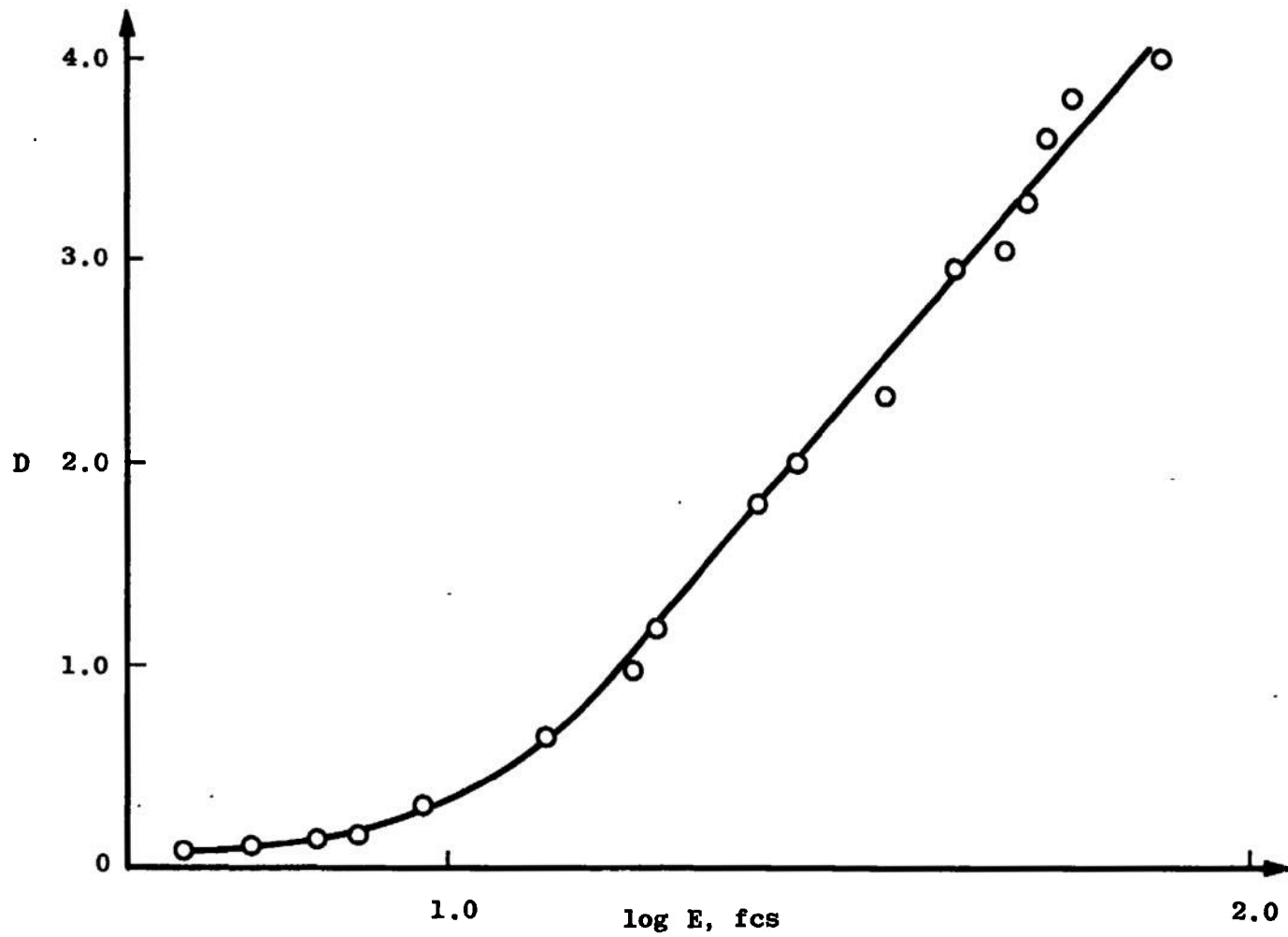
(a) H and D curve

Figure 6. Characteristic curves of the film used to
fabricate the filter A'(x_f).
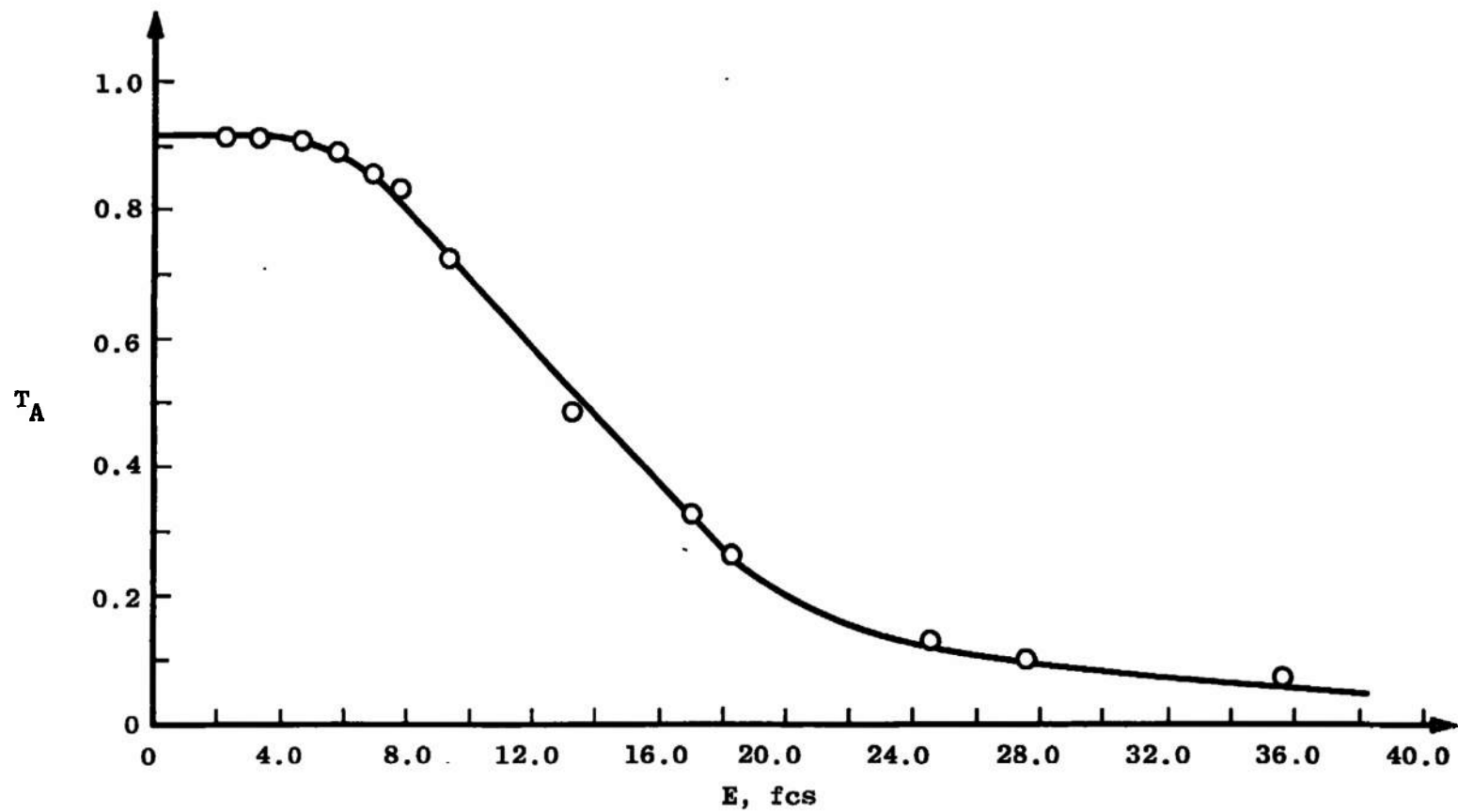
(b) Amplitude transmission versus exposure curve

Figure 6. (continued)

$$v_1 = \pm \, 111.5 \, t^{-3.29} \text{ cm/sec} \tag{44}$$

A plot of the velocities and distances as a function of exposure is shown in Figure 7. The velocity v_o is easily seen to occur at $t = 4.3$ seconds or at an exposure of 16.15 fcs. Since the maximum density of four could be measured, the maximum exposure time is 20 seconds.

The edges travel from $\pm \, 0.05$ cm to $\pm \, 5$ cm in a period of 20 seconds, which is shown in Figure 7(a). For making the filter $A'(x_f)$, the entire distance of 10 cm is imaged on the film by a camera with a magnification of 1/10th. The filter
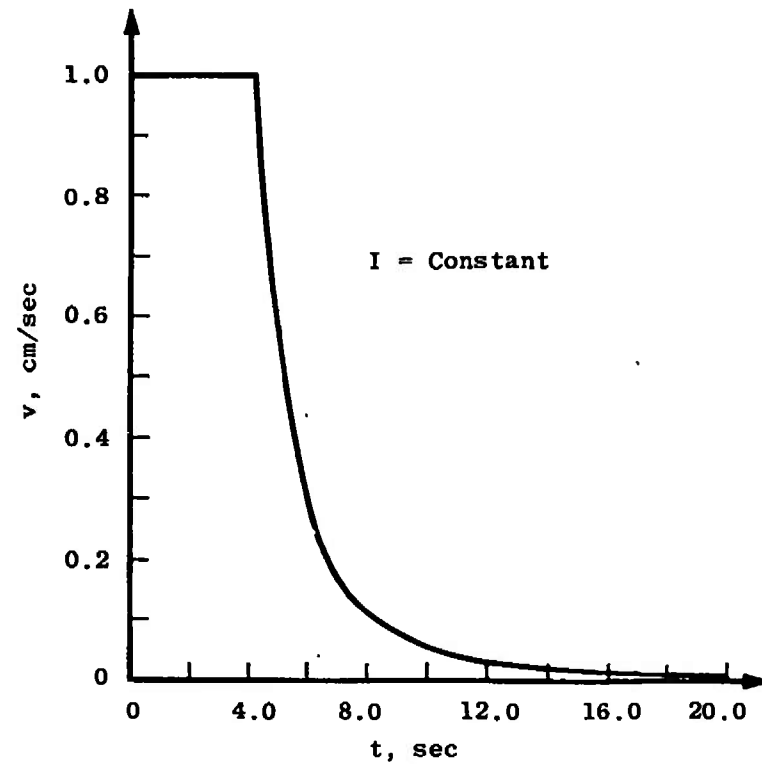
$$A'(x_f) = \left| \frac{x_f}{5} \right| \tag{45}$$

has a density curve as shown in Figure 8. The density of four from -0.05 mm to +0.05 mm is used to block the spatial frequency of $0 \leq |\omega| \leq B$.

The velocities that the edges must have to vary the exposure are known from the velocity-exposure curve of Figure 7(b). The apparatus used to move the edges at the correct velocities is called a filter generator and it is shown in Figure 9. A permanent magnetic D. C. motor was chosen for the filter generator since it has a linear relationship between the voltage input and the motor speed (RPM). In order to have the correct velocity-exposure curve
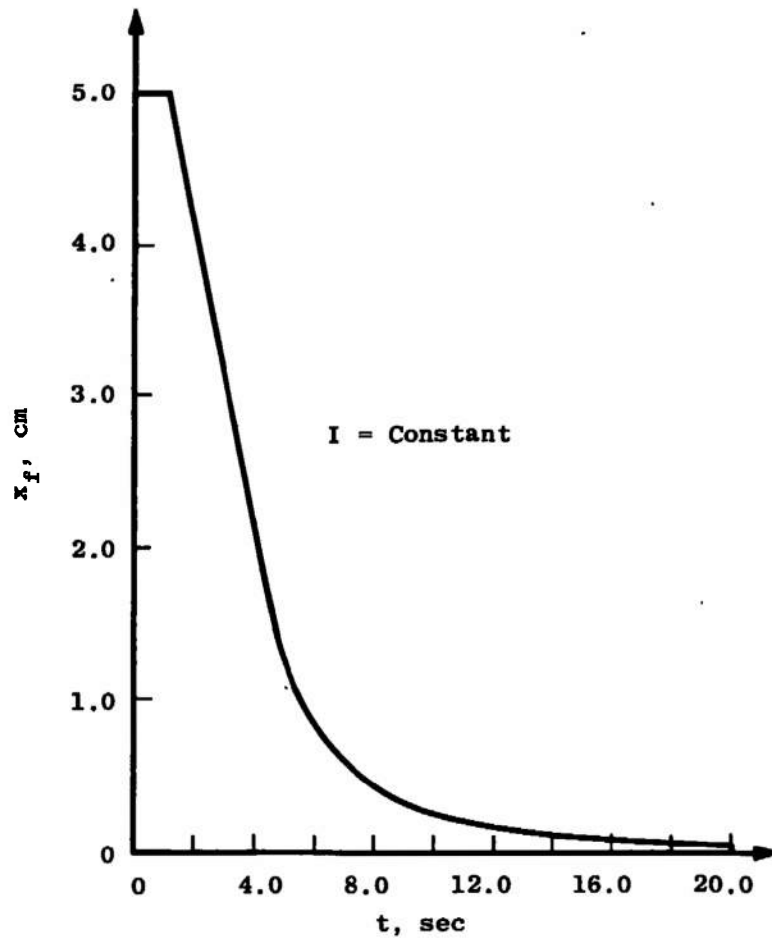
(a) Distance-exposure curve   (b) Velocity-exposure curve
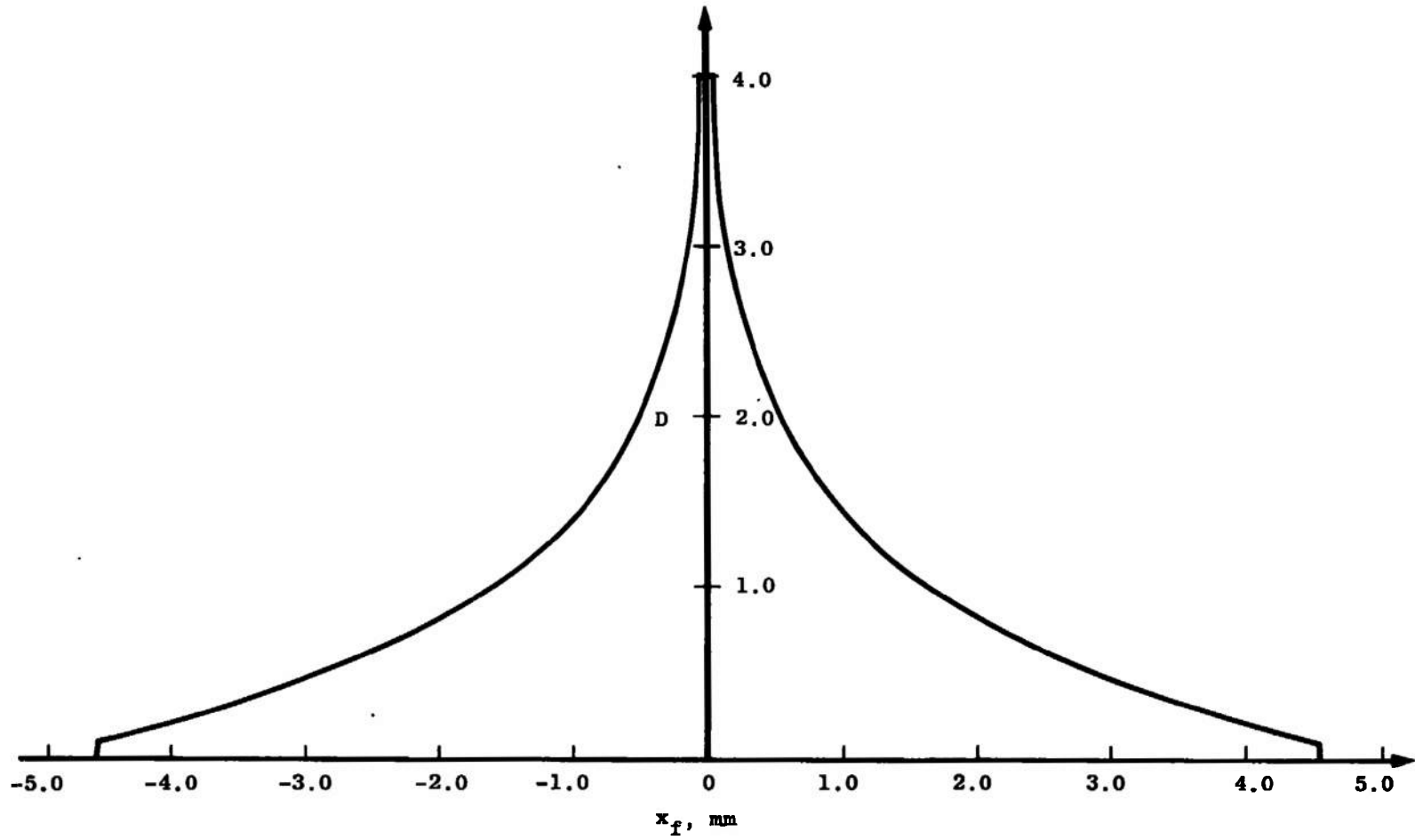
Figure 7. The exposure curves for the filter A'(x_f).

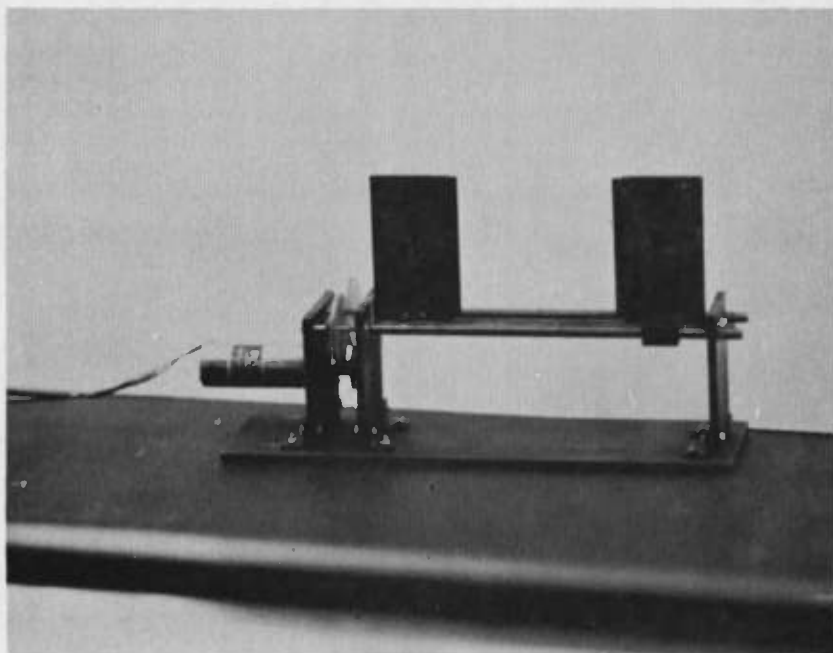Figure 8.   Density plot of the filter A'(x_f).

Figure 9. Filter generator.

output at the edges, a voltage-exposure relation was found in terms of the input to the D. C. motor. The input voltage versus the RPM output of the D. C. motor is shown in Figure 10. It is described by the equation

$$V_{DC} = (0.046)(RPJ) + 1.4 \text{ vdc} \tag{46}$$

The rpms of the D. C. motor are converted by the filter generator to the desired edge velocities.

The output of the D. C. motor is geared down by 12/19. The edges are mounted on threaded rods with 16 threads/inch, and the threaded rods are connected to the gears. These threaded rods convert the rotation of the motor's shaft to lateral displacement of the edges. The edges are displaced one inch for every 16 revolutions of the thread rods. The velocity of the edges is expressed in terms of the D. C. motor speed as

$$v = [\frac{12}{19}] [\frac{(2.54 \text{ cm/in.})(RPM)}{(60 \text{ sec})(16/\text{in.})}]$$

$$= 1.675 \times 10^{-3} \text{ RPM cm/sec}$$

or

$$RPM = (5.975 \times 10^2)v \tag{47}$$

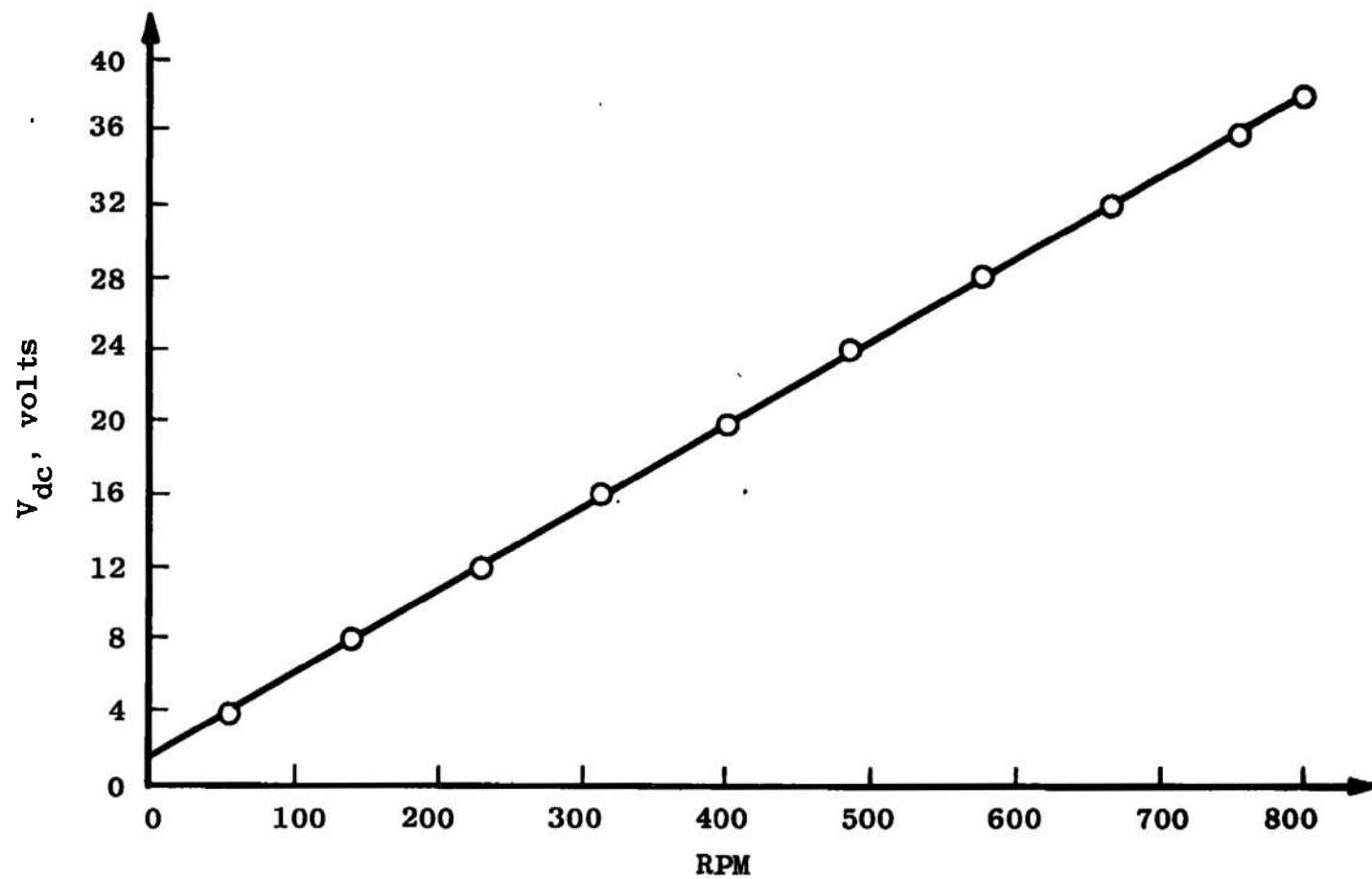Therefore, for the voltage input to the motor in terms of the edge velocity,

Figure 10.   Velocity characteristics of the D. C. motor.

$$V_{DC} = (27.55 \text{ v} + 1.4) \text{ vdc} \qquad (48)$$

From Equation (48) and Figure 7, page 26, it is noticed that
the edge velocities less than 0.11 cm/sec are beyond the
continuous capabilities of the D. C. motor since the break-
away rpm of the motor is 56 rpms. The edge velocities less
than 0.11 cm/sec are obtained by pulsing the D. C. motor
with a voltage pulse. The pulse motor control is simply a
rotating switch which has four contacts, and when the switch
is closed, a voltage is momentarily placed across the motor
terminals. Varying the voltage across the switch will vary
the speed of the motor. The curve for the relationship
between the pulse voltage and edge velocity is shown in
Figure 11 for the switch contacts rotating at 500 rpms.

The input to the D. C. motor is amplified by an
amplifier with a voltage gain of six and a current gain of
approximately 10^4. From Equation (48) and Figures 7 and 11,
the voltage-exposure curve is found, and it is shown in
Figure 12. The voltage-exposure curve generates the edge
velocity-exposure curve of Figure 7(b). The input to the
amplifier is the voltage-exposure curve. The period of the
voltage-exposure curve is 20 seconds. This waveform is
generated by a device called a function generator which is
shown in Figure 13. The waveform is generated by placing a
voltage across a 5000 ohms, 200 watt variable wirewound
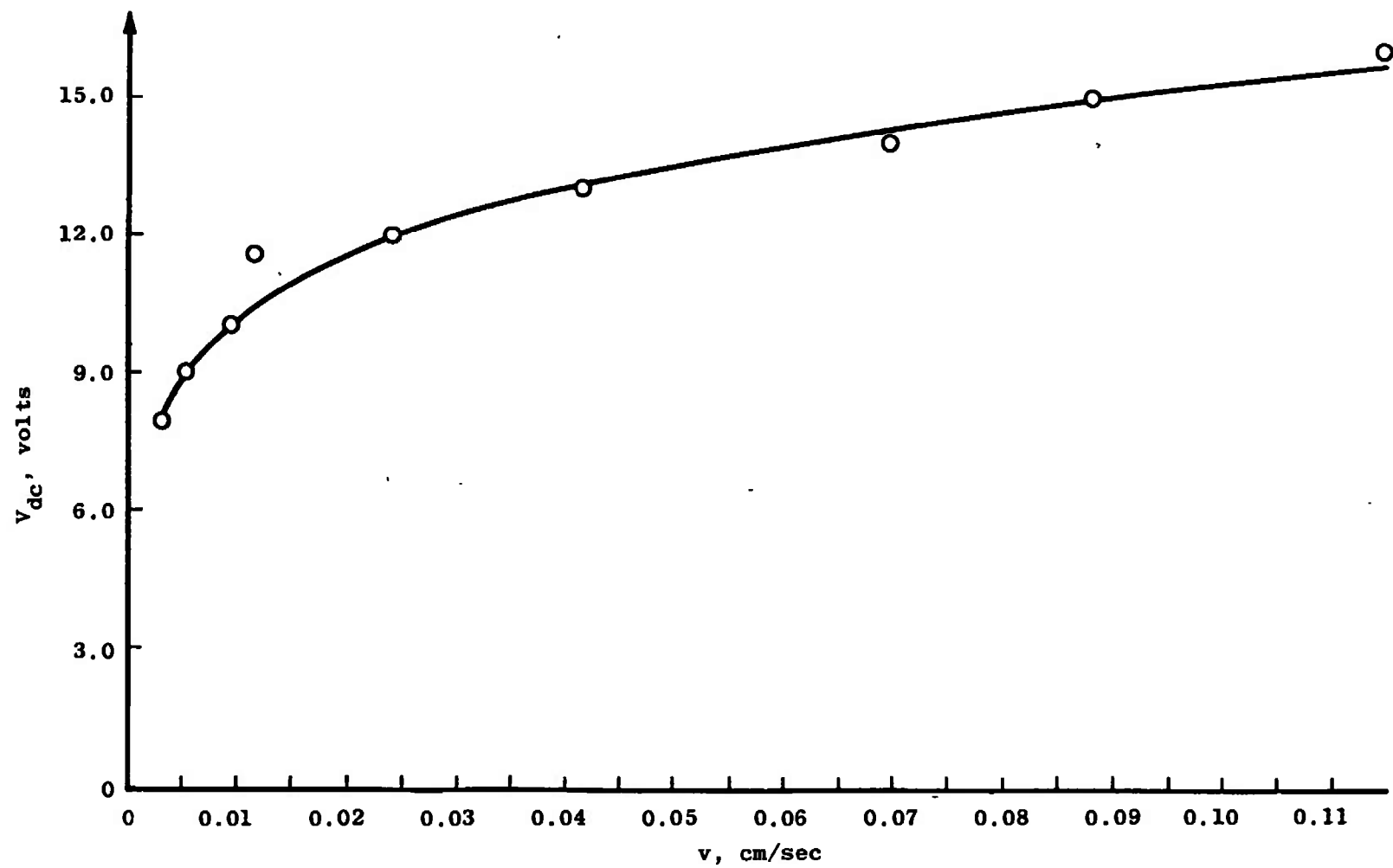resistor. The resistor is moved against a wire in the shape

32

Figure 11.   Input voltage versus edge velocity for pulse
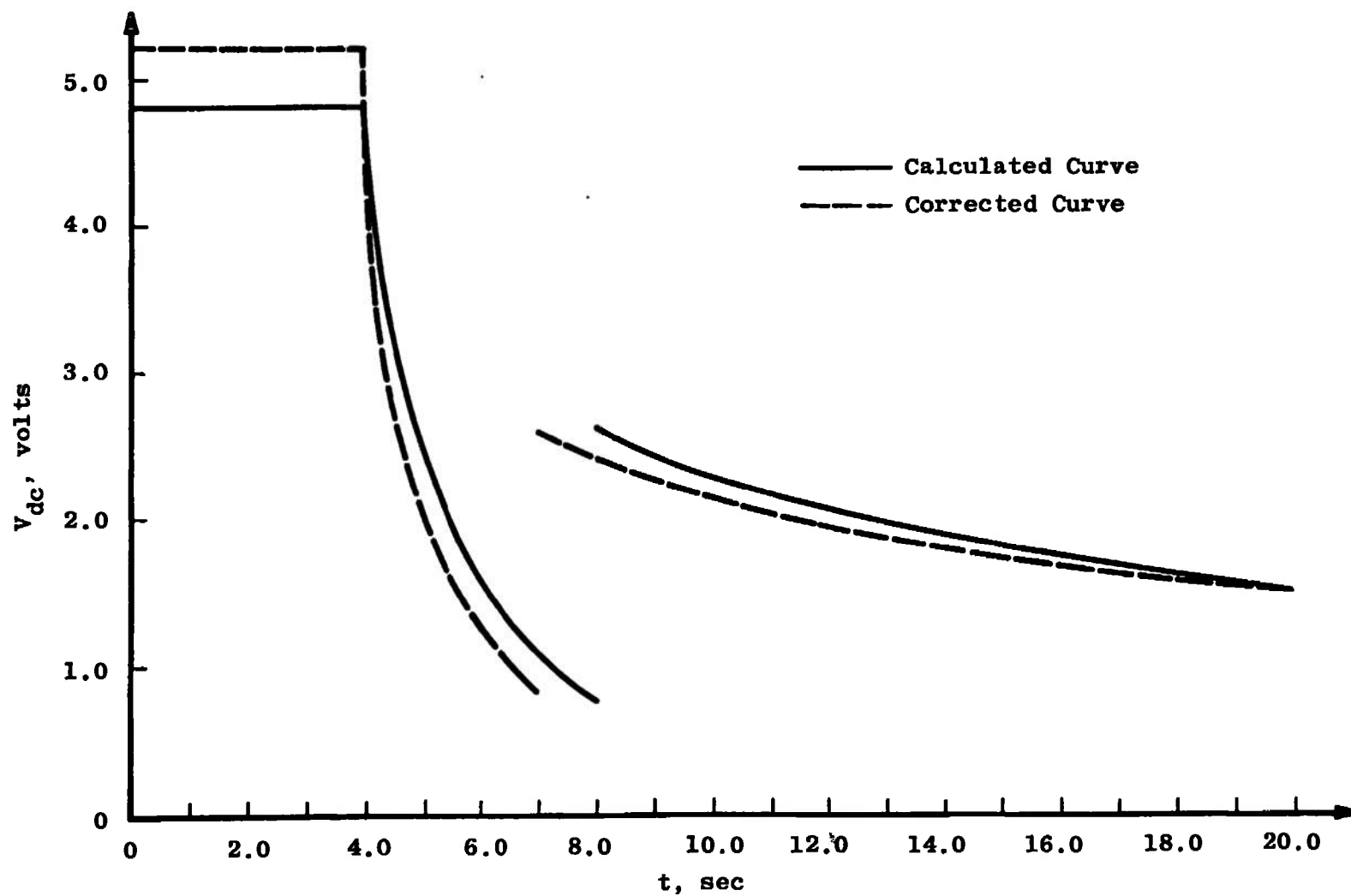   motor control.

Figure 12. Voltage-exposure curve for fabrication of the
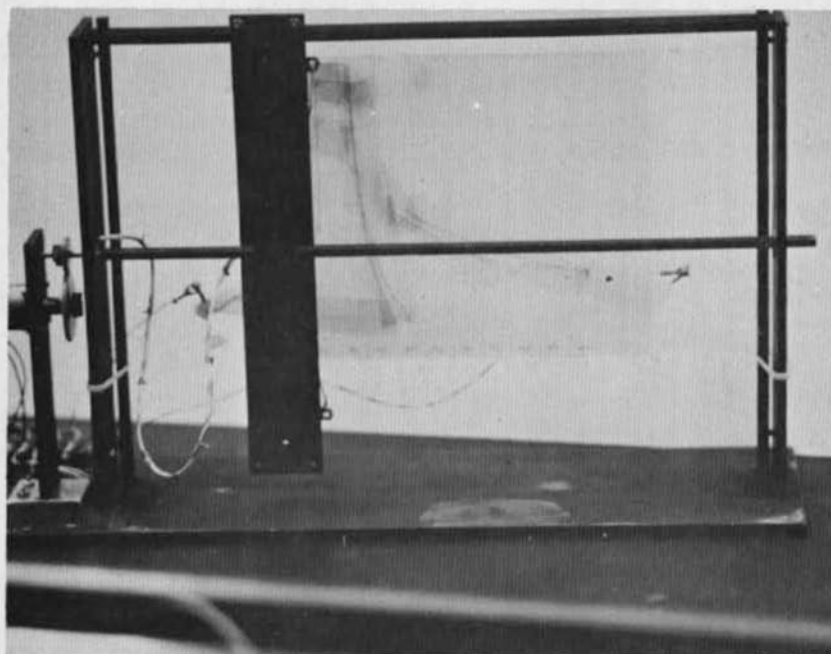   filter A'(x_f).

Figure 13.   Function generator.

of the voltage-exposure curve. Note presence of the wire in
Figure 13. The resistor is calibrated to give 0.25 volts/cm.
The resistor is moved 20 cm in 20 seconds by a D. C. motor
and a threaded rod. The amplifier, D. C. power supply
number 1 which drives the motor of the function generator,
and D. C. power supply number 2 which biases the resistor,
compose the power control unit. The block diagram demon-
strating the manner in which the filter $A'(x_f)$ is generated
is shown in Figure 14.

The amplitude transmission of the generated filter
$A'(x_f)$ is found by using a microdensitometer. For the first
filter attempted, the density was too high in the center and
too low at the ends because of the reciprocity effect. To
correct these errors, the voltage-exposure curve was changed
to the dashed curve shown in Figure 12. Then, the filter
$A'(x_f)$ was generated with the accuracy shown in Figure 15.
The deviation at the ends is again due to the reciprocity
effect which could not be overcome.

The Phase Filter $\theta(\omega)$

The phase filter $\theta(\omega)$ is made by depositing a
dielectric coating on glass. The dielectric coating thick-
ness is varied to give the desired phase shift. The index
of refraction of air is denoted as n_a , and n_b corresponds
to the dielectric coating. The index of refraction is
simply the ratio of the velocity of light in a vacuum, c, to
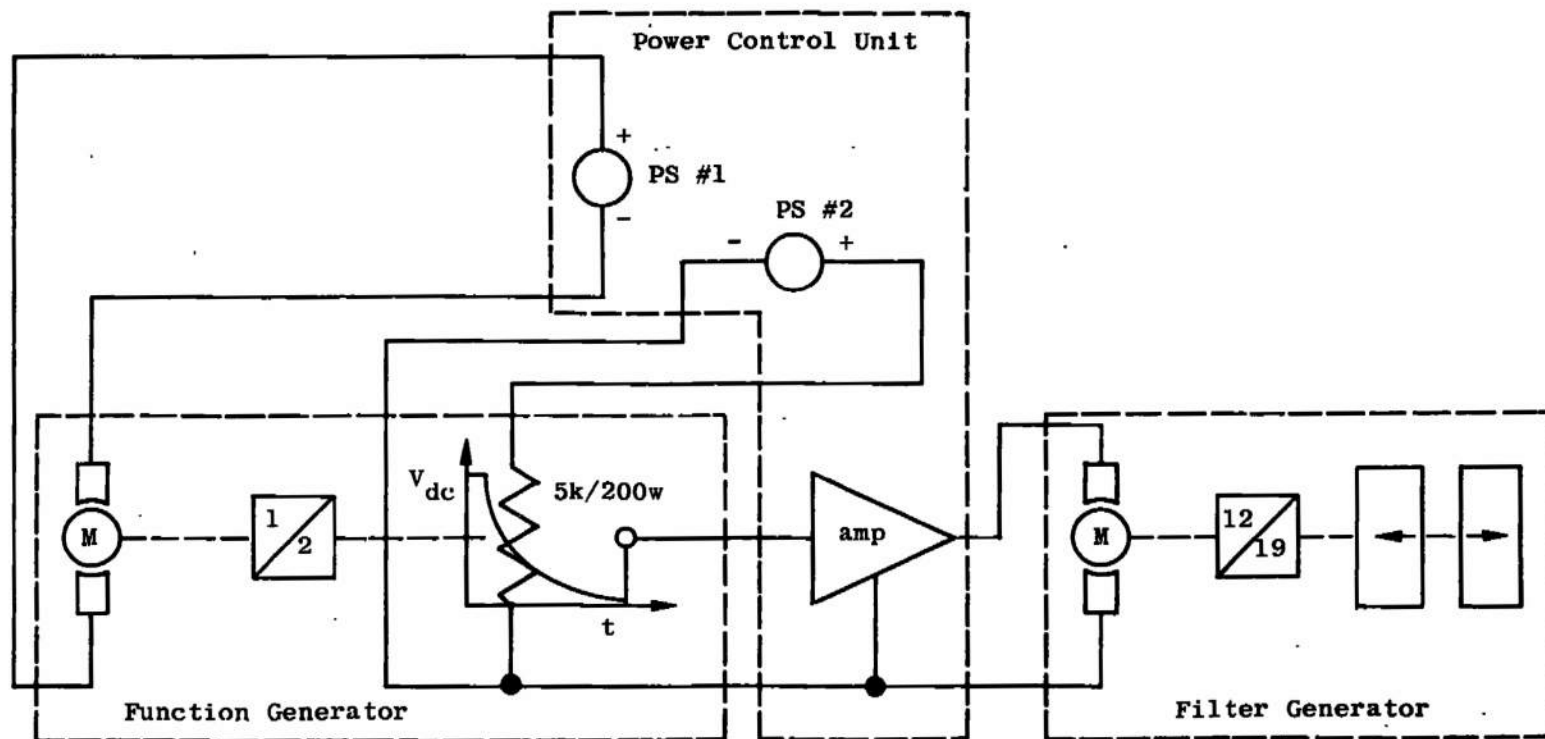the velocity of light in the medium, ν, or [10]

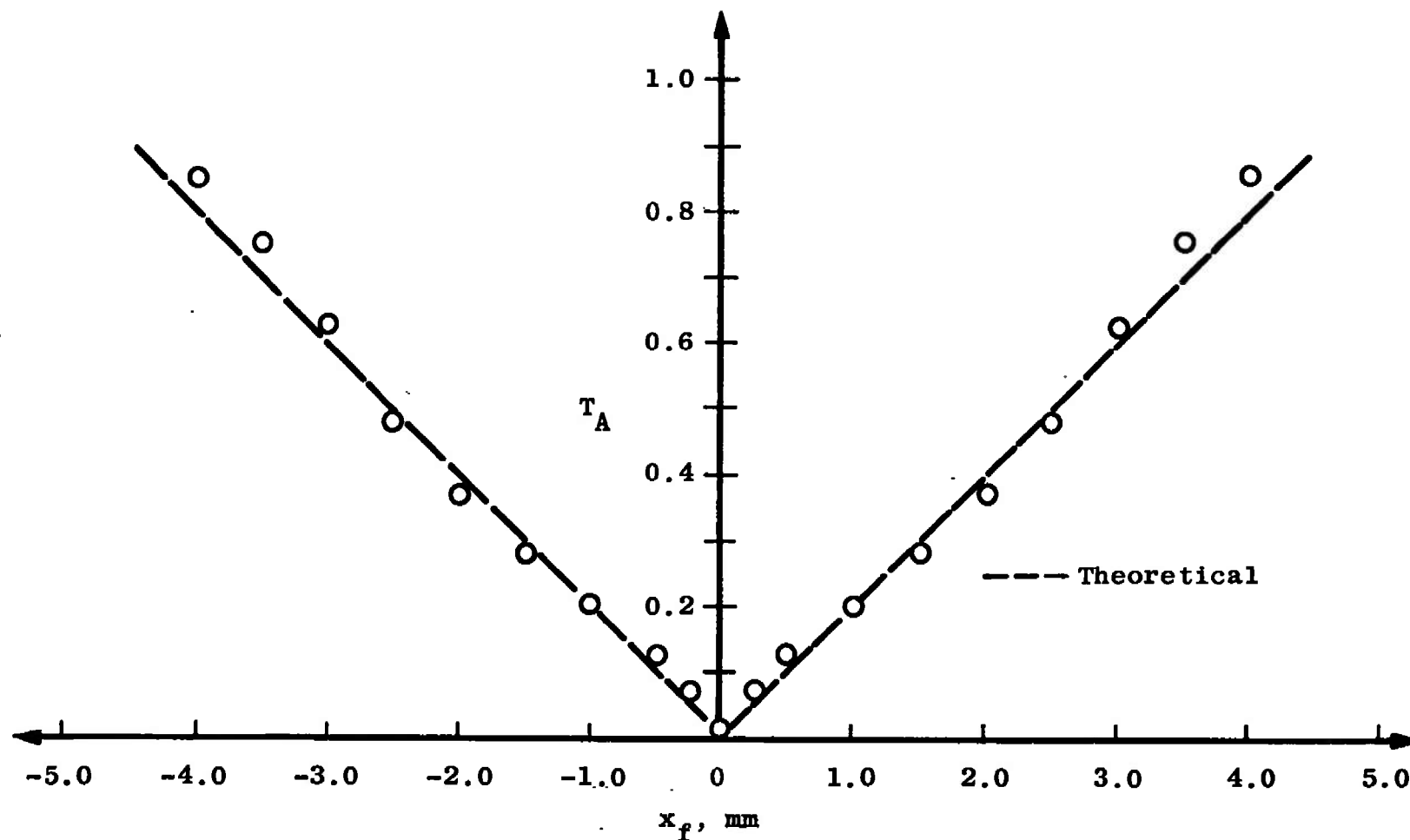Figure 14. Block diagram of apparatus used for generating the filter $A'(x_f)$.

Figure 15. Amplitude transmission versus distance for the
experimental filter A'(x_f).

$$n = \frac{c}{v} \qquad (49)$$

As seen from Figure 2, page 10, a phase of $-\pi/2$ radians and $+\pi/2$ radians is needed for the fabrication of the filter $\theta(\omega)$ which is a total phase difference of π radians between the positive and the negative half frequency plane. Therefore, a phase shift of π radians is only needed for the negative frequency. For the phase shift of π radians, the light wave must be delayed in the dielectric material by $\lambda/2$ with respect to light wave traveling in air. Hence,

$$\frac{\lambda}{2} = (v_a - v_b)t'$$

$$t' = [\frac{\lambda}{2c}][\frac{n_a - n_b}{n_b - n_a}] \qquad (50)$$

where t' is the time required for the light to travel a distance $\lambda/2$ in the dielectric material. Then the required thickness of the dielectric material is

$$d_n = v_b t'$$

$$= \frac{\lambda}{2}[\frac{n_a}{n_b - n_a}] \qquad (51)$$

Fabricating the phase filter. The required thickness of the dielectric coating is deposited on one half of a

39

one-inch square glass plate. To measure the amount of dielectric deposited on the glass, the reflectivity of the dielectric material on the glass is measured. The reflectivity as a function of wavelength thickness will resemble Figure 16 [10]. The one-inch square glass plate is placed on top of a stand inside a bell-shaped vacuum chamber. One-half of the glass plate is blocked by a sheet of metal. The dielectric material is deposited by heating it to a high temperature at the bottom of the stand. Due to the shape of the vacuum chamber, the light source used to measure the thickness of the dielectric is incident upon the glass plate at 45°. The light source is a He-Ne laser. Therefore, the thickness measured by the reflectivity is at an angle of $\pi/4$ radians. Hence, the normal thickness, d_n , is

$$d_n = 0.707 \ d_{\pi/4} \tag{52}$$

The dielectric material, silicon mono-oxide, SiO, is used. Its index of refraction is

$$n_b = 1.97 \tag{53}$$
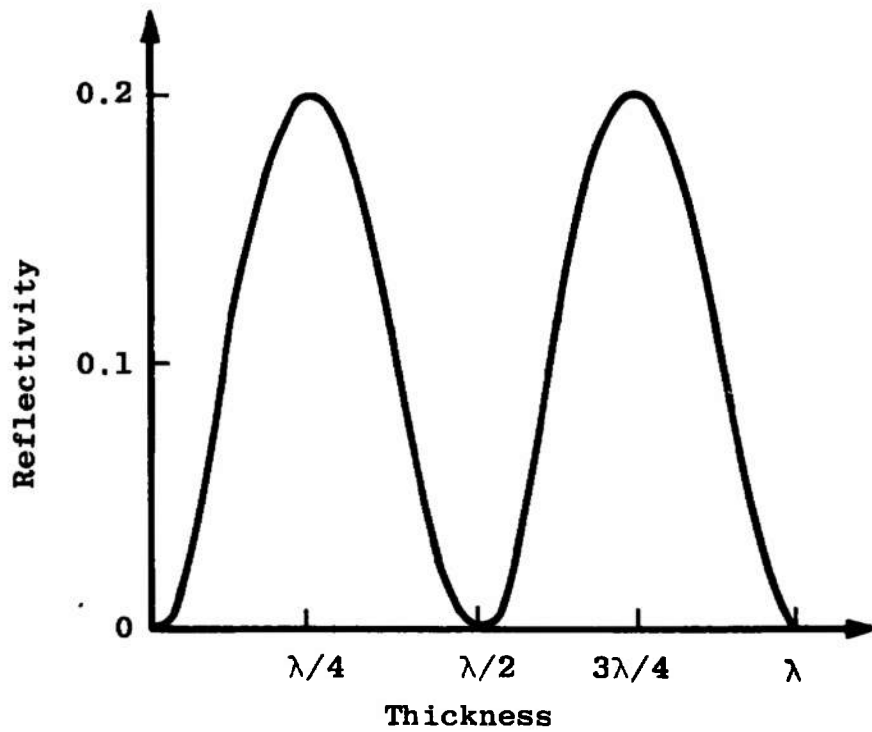
then

$$d_n = 0.516\lambda \tag{54}$$

Figure 16. The reflectivity of a dielectric coating on glass for $n_b = 2.0$.

Since only $d_{\pi/4}$ thickness is measured, the dielectric coating is stopped when the thickness

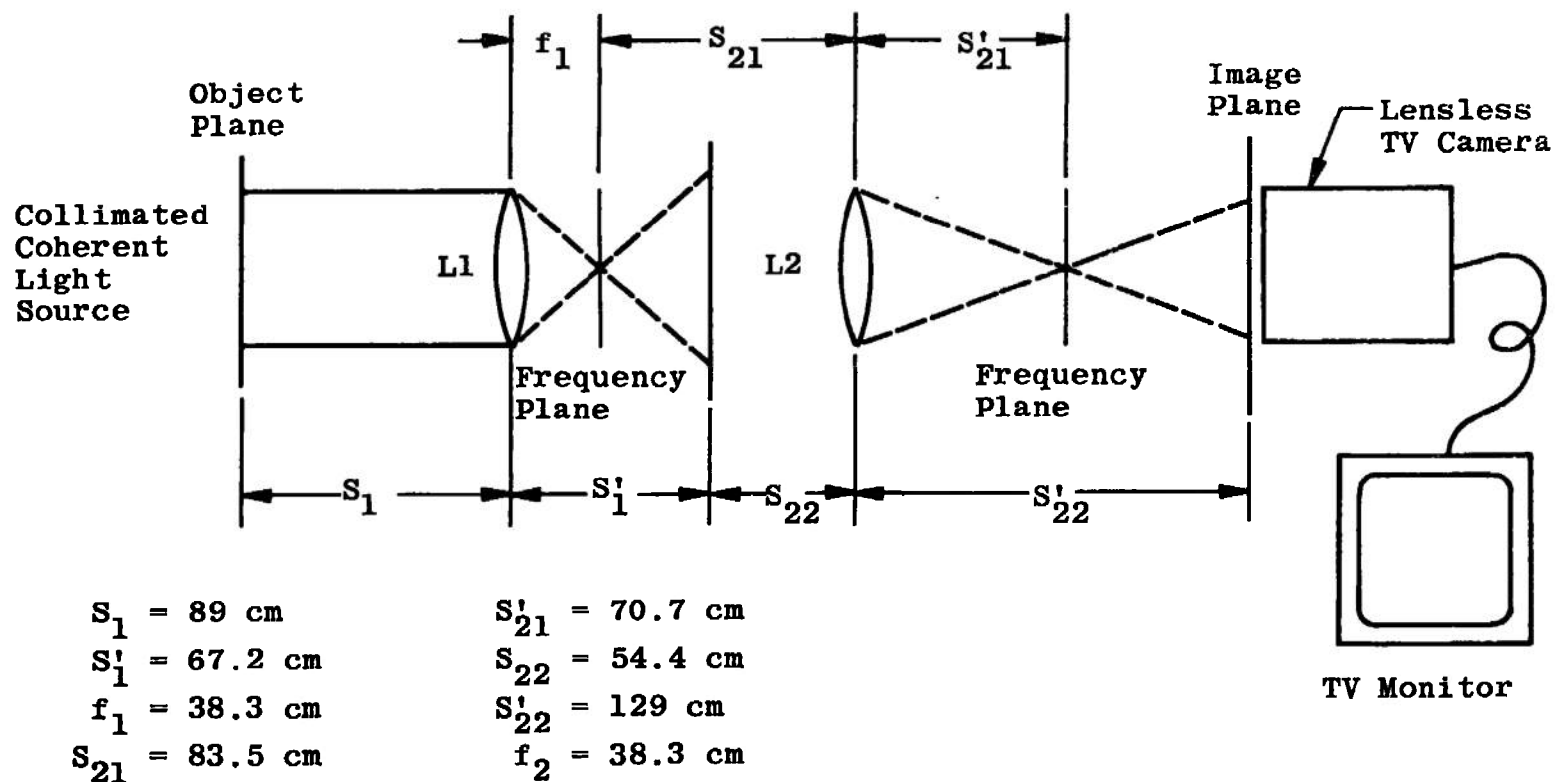$$d_{\pi/4} = 0.74\lambda \qquad (55)$$

is reached.

CHAPTER III

EXPERIMENTAL COMPARISONS OF VARIOUS

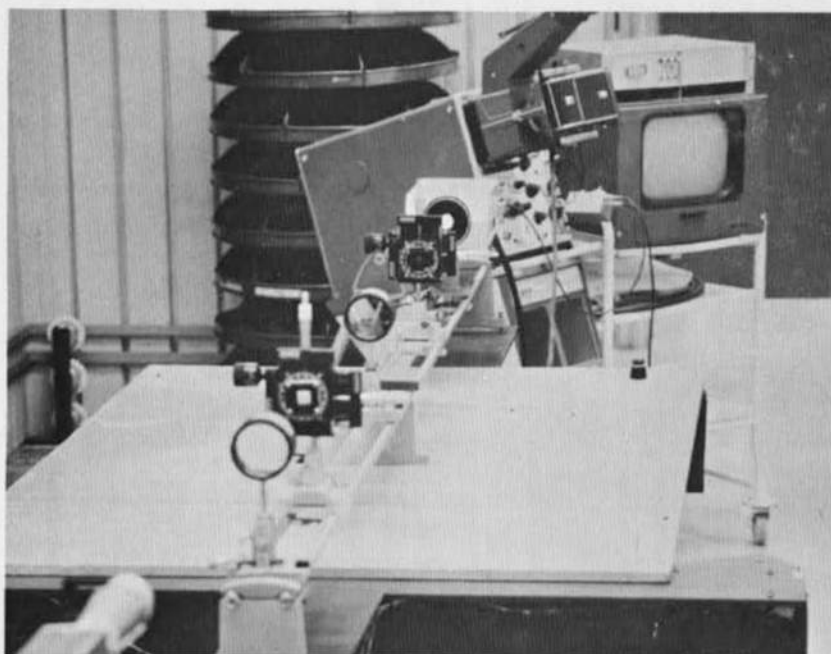OPTICAL FILTERING METHODS

I. INTRODUCTION

Experiments are constructed to test the charac-
teristics of various optical filters. The diagram of the
test apparatus is shown in Figure 17(a). The TV system is
used to view the image plane; it is a high resolution system
of a 1000 horizontal scan lines per vertical scan with a
bandwidth of 32 MHz. To examine closely the effect of ·
optical filtering on the input, a portion of a single hori-
zontal scan line of the TV system is viewed on an
oscilloscope; this relates to a cross section of the
intensity pattern in the image plane. The oscilloscope used
is a Tektronix 547 with a 1A5 preamp yielding an oscillo-
scope rise time of 8 nsec. Therefore, the combination of
the oscilloscope and the TV system has a rise time of 13.6
nsec. The TV system was calibrated so that the distance
could be measured from the time scale of the oscilloscope.
The relationship is 131.0 $\pm$ 4.65 microns/cm for a time
scale of 0.2 µsec/cm for unity magnification.

The ability of the various filters to minimize the
error in the location of an edge is tested using a step

S_1 = 89 cm S'_{21} = 70.7 cm

S'_1 = 67.2 cm S_{22} = 54.4 cm

f_1 = 38.3 cm S'_{22} = 129 cm

S_{21} = 83.5 cm f_2 = 38.3 cm

(a) Diagram

Figure 17.   Filter test apparatus.

(b) Photograph of experiment

Figure 17.   (continued)

function. In addition, several of the filters are applied
to phase information for comparison of the various filtering
techniques.

II. THE STEP FUNCTION

The input used to test the response of the
different optical filters is a one-dimensional step function
which is the edge of a razor blade. The step function has
an amplitude transmission of

$$s(x_o) = \frac{1}{2} (1 + \text{sgn } x_o) \tag{56}$$

Then,

$$\mathcal{F}\{s(x_o)\} = S(\omega)$$

$$= \frac{1}{2} [\delta(\omega) + \frac{1}{j\omega}] \tag{57}$$

The step function is imaged on the vidicon, but it is not a
perfect step function due to bandlimiting by the optics.
The image intensity of the step function is [12]

$$I_i(x) = [\frac{1}{2} + \frac{1}{\pi} \text{Si}(\frac{\kappa bx}{2q})]^2 \tag{58}$$

where q is the image distance, b is the radius of the lens,
and $\kappa = 2\pi/\lambda$. The curve generated by Equation (58) is shown
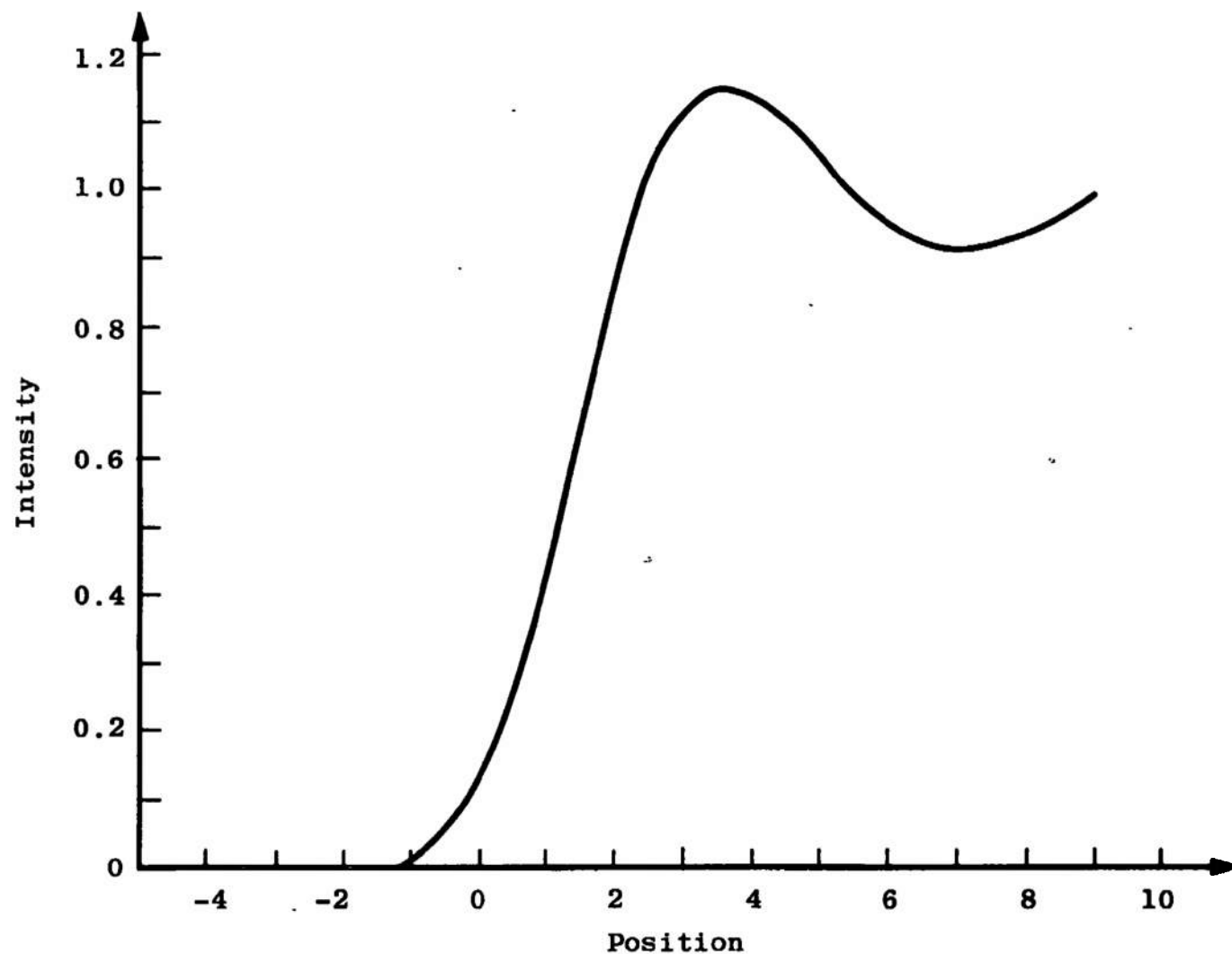in Figure 18.

Figure 18. Image intensity of a step function bandlimited by a lens.

A portion of a horizontal scan line showing the intensity cross section of the step function in the image plane is shown in Figure 19. The rise time of the step function is 80 nsec which is slower than the rise time capability of the electronic system. This indicates that the electronic system gives a reasonably accurate display of the signals in the image plane. The rise time of the step function is therefore due to bandlimiting effects as described by Equation (58).

For comparison of the different optical filters, the manual gain of the TV system was maintained constant. Referring to Figure 17(a), page 44, lens L2 magnifies the transform plane of lens L1 by 0.845, but the overall magnification of the object plane by lens L1 and L2 is 1.79. A He-Ne laser is used for the coherent light source; therefore, in the frequency plane of lens L1, each centimeter represents a spatial frequency of 4.13×10^3 lines/mm and in the frequency plane of lens L2, 3.49×10^3 lines/mm. Due to the magnification of the object plane, the relationship of the distance and time base is 33.8 ± 1.3 microns/cm for an oscilloscope time scale of 0.1 μsec/cm, respectively.

The step function is attenuated by a neutral density filter with an intensity transmission of 0.0467; hence, the amplitude of the step function is 4.28v instead of 200 mv as shown in Figure 19(a). These values of voltages are read off the oscilloscope and are proportional
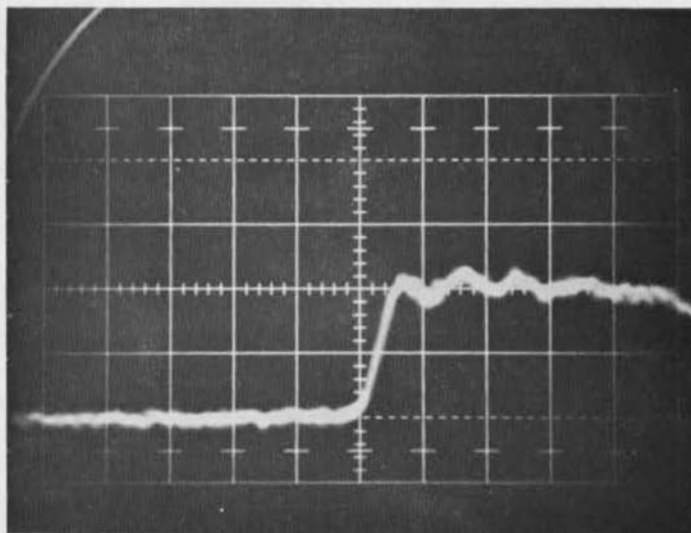
y axis: 100 mv/cm   x axis: 0.1 μsec/cm

(a) A horizontal scan line of the image plane
    attenuated by a neutral density filter
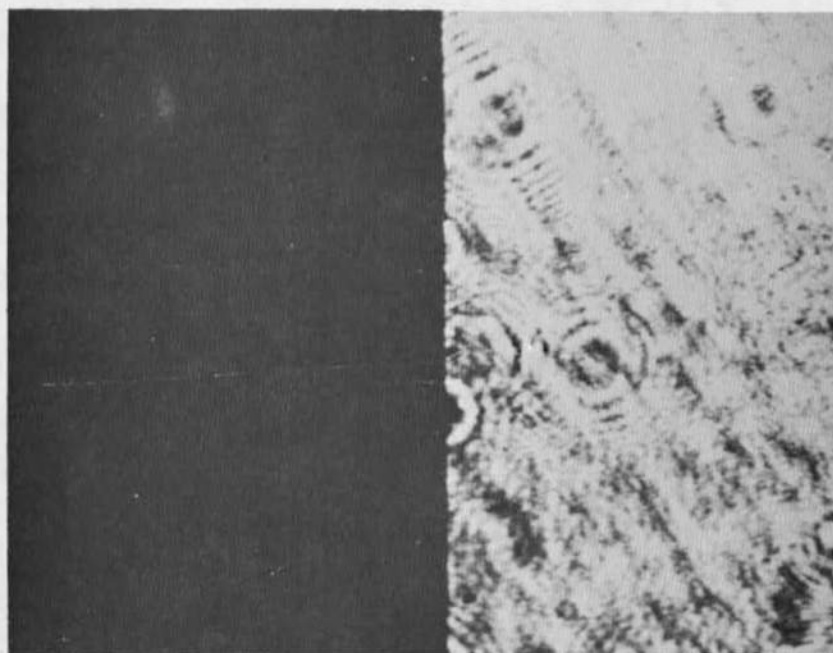
(b) The image plane as viewed on the TV monitor

Figure 19.   The bandlimited step function.

to the intensity incident upon the vidicon active surface.
They are relative values only.

III. THE DERIVATIVE OF THE STEP FUNCTION

The derivative of the step function is taken by
placing the phase filter, $\theta(\omega)$, in the frequency plane of
lens L1 and the linear amplitude filter, $A'(\omega)$, in the
frequency plane of lens L2 to yield the filter $F'(\omega)$. The
filter $A'(\omega)$ has dimensions of 7 mm x 7 mm, and the phase
filter $\theta(\omega)$ has dimensions of 2.4 cm x 2.4 cm. The spectrum
of the frequency plane of lens L2 is shown in Figure 20.
From Equation (13), the intensity of the bandlimited
derivative of a step function is

$$I(x_i) = 4 \, A_{max}^2 k^2 (W-B)^2 \left[sinc((W-B)x_i) \cos\left(\left(\frac{W+B}{2}\right)x_i\right) \right]^2 \qquad (59)$$

A portion of the horizontal scan line in Figure
21(a) shows the intensity of the bandlimited derivative; its
maximum amplitude is 130 mv. The rise time of the deriva-
tive is slower than the rise time of the step function.
This is due to the derivative having an upper bandlimiting
frequency, W. This frequency is much smaller than the
limiting frequency, b, of the step function. The band-
limited derivative of the step function is 108 microns wide.
The maximum error in locating the edge is 54 microns.

The manual gain of the TV system was increased,
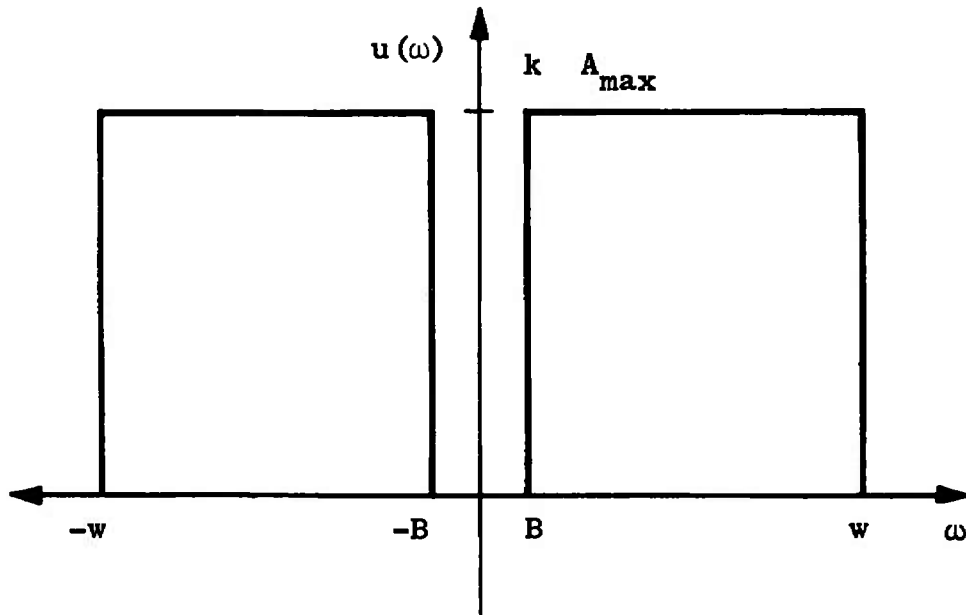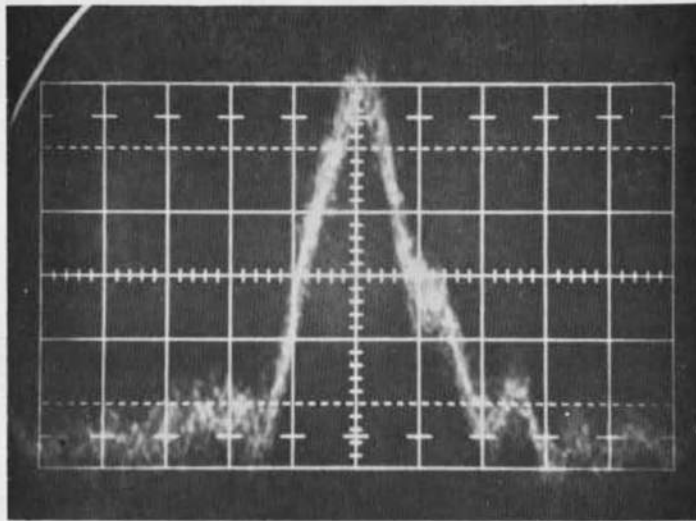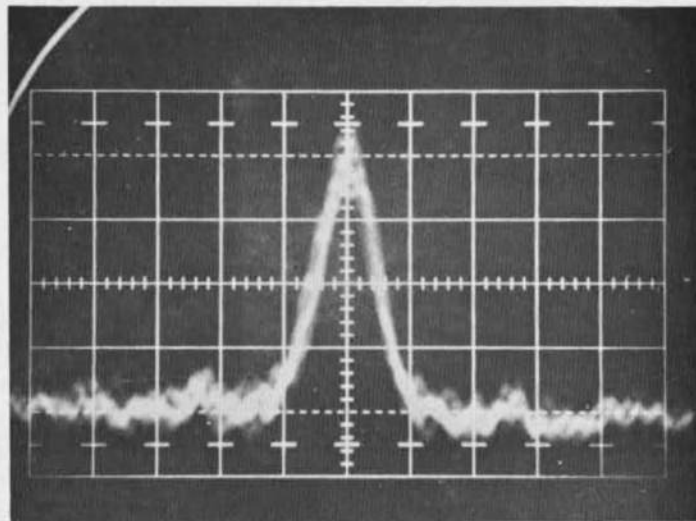and the derivative of the step function is shown in

Figure 20. The frequency spectrum for the step function
filtered by the filter F'(ω).

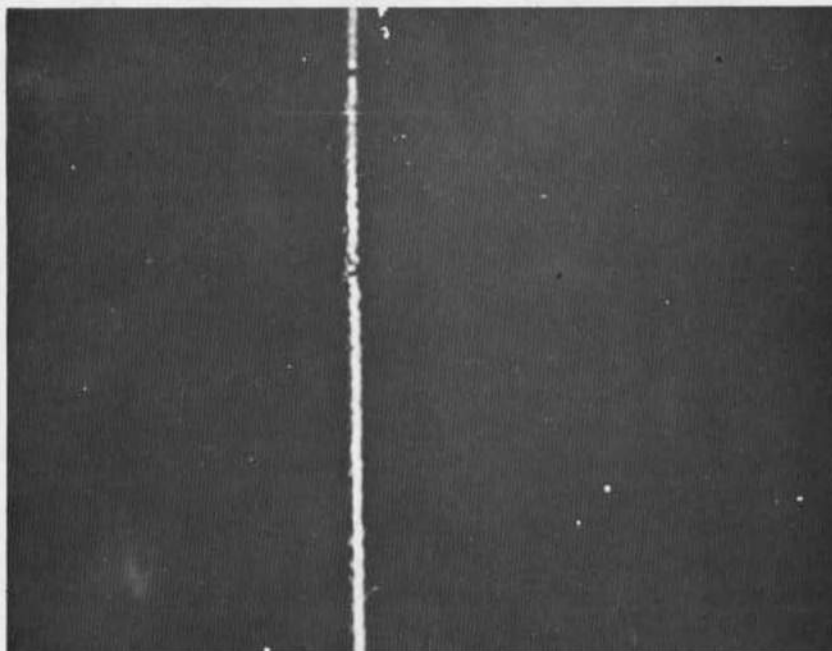y axis: 20 mv/cm   x axis: 0.1 μsec/cm

(a) A horizontal scan line of the image plane

y axis: 100 mv/cm   x axis: 0.1 μsec/cm

(b) A horizontal scan line of the image plane for
    the manual gain increased

Figure 21.   The bandlimited derivative of the step function.

(c) The image plane as viewed on the TV monitor

Figure 21. (continued)

Figure 21(b). The increase in gain increases the amplitude of the signal and increases the signal-to-noise ratio.

The filter F'(ω) is rotated in the frequency plane and the derivative of the step function is shown to conform to Equation (17) by Figure 22. It is impossible to demonstrate the derivative as a function of the magnification since the amount of energy per unit area changes in the image plane as a function of the magnification which causes changes in the signal amplitude.

IV. FILTERING OF THE STEP FUNCTION BY THE LINEAR AMPLITUDE FILTER

The filter A'(ω) was discussed in Chapter II. Its amplitude transmission is shown in Figure 4, page 16. The filter A'(ω) filters the step function in the frequency plane of lens L2; the frequency spectrum is shown in Figure 23. This frequency spectrum is simply

$$U(\omega) = k \, A_{max} \, \text{rect} \, [\frac{\omega + \frac{W+B}{2}}{W-B}] e^{+j\frac{\pi}{2}}$$

$$+ k \, A_{max} \, \text{rect} \, [\frac{\omega - \frac{W-B}{2}}{W-B}] e^{-j\frac{\pi}{2}} \tag{60}$$
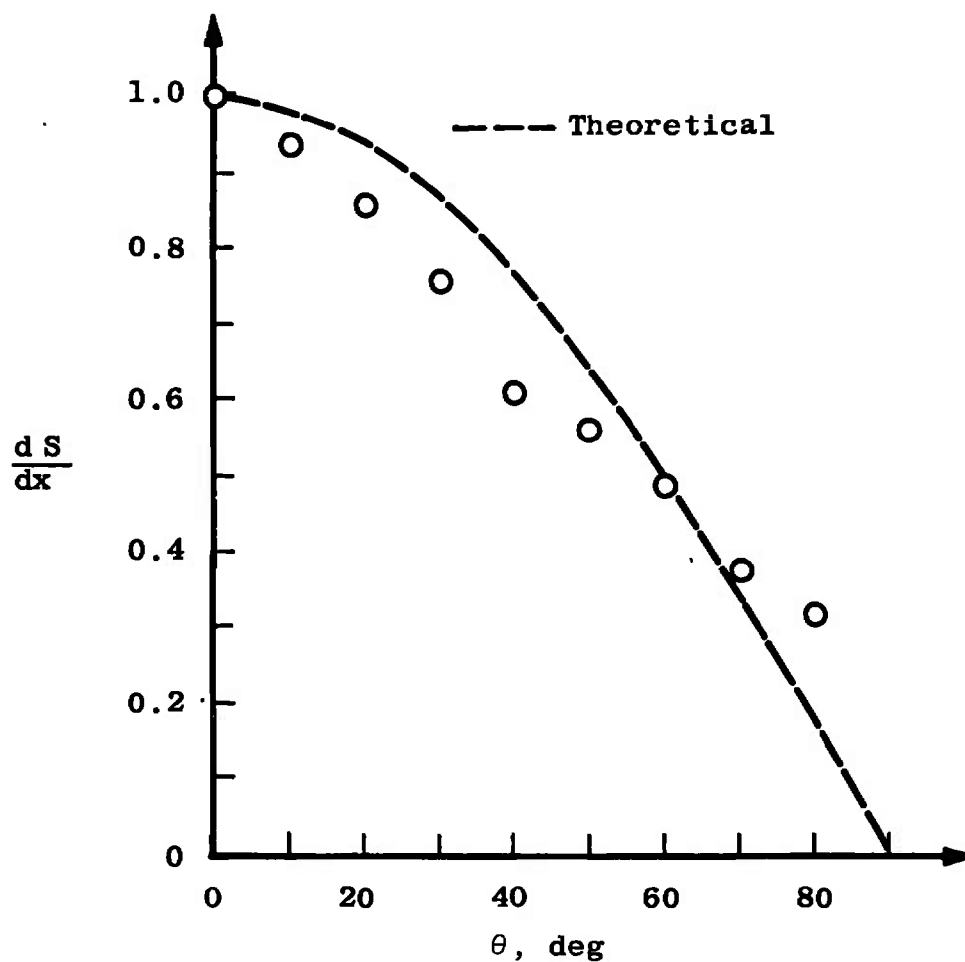
Then the amplitude in the image plane is

Figure 22.   The bandlimited derivative of the step function
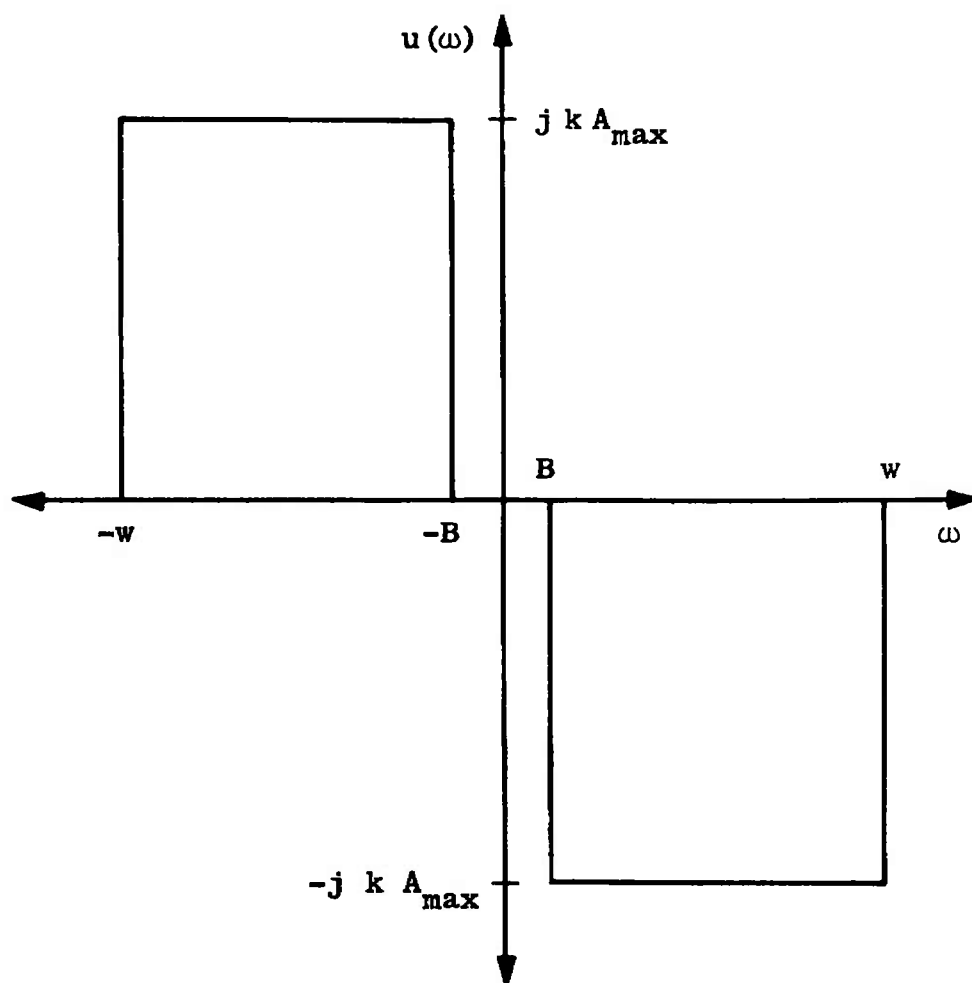as a function of the angle θ.

Figure 23.   The frequency spectrum for the step function
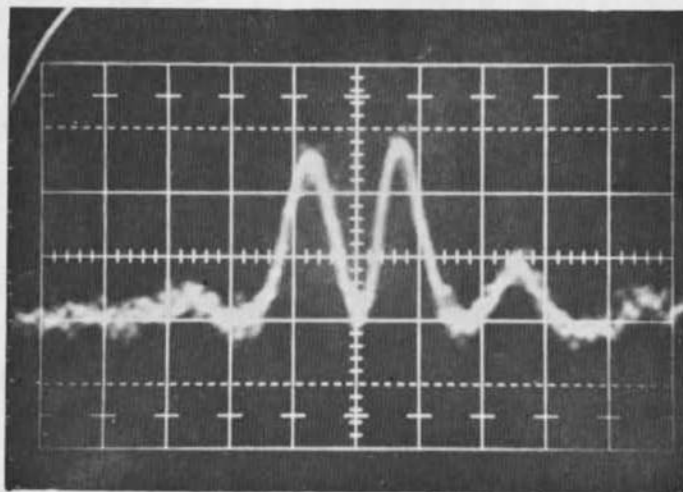   filtered by the filter $A'(\omega)$.

$$\mathcal{F}\{U(\omega)\} = U(x_i)$$

$$= jk\, A_{max}\,(W-B)\,[sinc[(W-B)_{xi}]e^{-j(\frac{W+B}{2})}$$

$$- sinc[(W-B)x_i]e^{+j(\frac{W+B}{2})}\,]$$

$$= 2A_{max}\,k(W-B)\,[sinc[(W-B)x_i]sin[(\frac{W+B}{2})x_i]] \qquad (61)$$

The intensity in the image plane is

$$I(x_i) = 4k^2\,A_{max}^2\,(W-B)^2\,[sinc[(W+B)d_i]sin[(\frac{W+B}{2})x_i]]^2 \qquad (62)$$

Notice that the only difference between Equations (62) and (59) is a sine and cosine function.

The intensity of the step function filtered by $A'(\omega)$ is seen in Figure 24. The "valley" in the horizontal scan line is caused by the sine function in Equation (62) since the sine is zero at $x_i = 0$. This "valley" is used to locate the edge of the razor blade. The "valley" is 40.7 microns wide; hence, the error in locating the edge is 20.35 microns. The maximum amplitude of Equation (62) in Figure 24 is 150 mv.

y axis: 50 mv/cm   x axis: 0.1 μsec/cm

(a) A horizontal scan line of the image plane
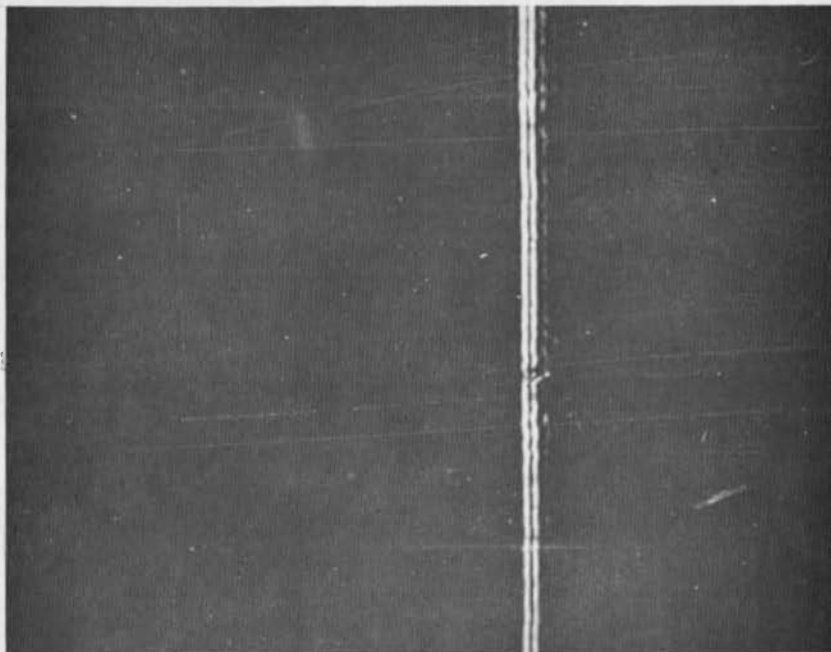
(b) The image plane as viewed on the TV monitor

Figure 24.   The step function filtered by the filter A'(ω).

V. THE HILBERT TRANSFORM METHOD APPLIED

TO THE STEP FUNCTION

The Hilbert transform is defined as [2]

$$\hat{U}_o(x_o) = \frac{1}{\pi} \int_{-\infty}^{\infty} \frac{U_o(x')}{(x_o - x')} \, dx' \tag{63}$$

The Hilbert transform filter is described by

$$H(\omega) = -j \, \text{sgn}(\omega) \tag{6}$$

This filter is constructed the same as the phase filter, $\theta(\omega)$. Therefore, the filter, $\theta(\omega)$, is used to take the Hilbert transform of a function in the object plane. For finding the Hilbert transform of the step function, the step function is represented by a rectangular pulse in the object plane; this is allowed since the collimated coherent light incident upon the object plane is not infinite in area. Then the Hilbert transform of the rect function

$$s'(x_o) = A \, \text{rect}\left(\frac{x_o}{\tau}\right) \tag{64}$$

is

$$\hat{s}'(x_i) = \frac{A}{\pi} \ln \left| \frac{x_i - \frac{\tau}{2}}{x_i + \frac{\tau}{2}} \right| \tag{65}$$

$\hat{s}'(x_o)$ denotes the Hilbert transform. The plot of

Equation (65) is shown in Figure 25. The edge of the razor
blade is located at $-\tau/2$. The portion of the horizontal
scan line showing the edge at $-\tau/2$ in the image plane is
shown in Figure 26(a). The width of the Hilbert transform
of the razor blade edge is 330 microns. This appears
visually as a smear of the razor blade edge. The maximum
error in locating the edge is 165 microns. The signal
amplitude is attenuated by a neutral density filter with
intensity transmission of 0.0467; therefore, the maximum
signal amplitude is 5.35 volts.

VI. THE SCHLIEREN METHOD APPLIED TO
THE STEP FUNCTION

Filtering by the Schlieren method is achieved by
introduction of a razor blade edge into the frequency plane
to block one half the frequency spectrum. This filter is
applied to the step function in the frequency plane of lens
L2. The Schlieren method filter is described as

$$T(\omega) = \frac{1}{2}(1 + \mathrm{sgn}(\omega)) \tag{4}$$

When this filtering is applied to the step function, the
image plane amplitude is [1]

$$U_i(x_i) = \frac{1}{2}[s_o'(x_i) + \frac{j}{\pi} \int_{-\infty}^{\infty} \frac{s_o'(x')}{(x_i - x')} \, dx']$$
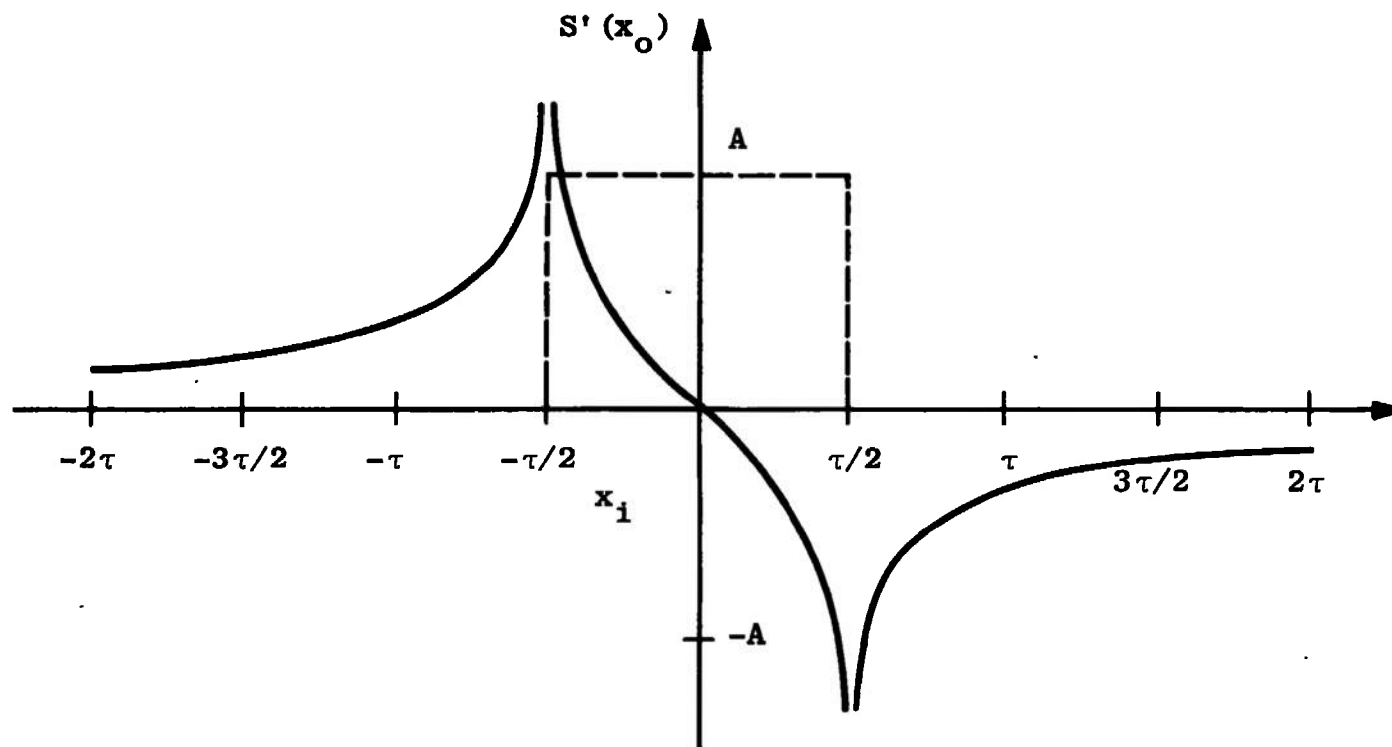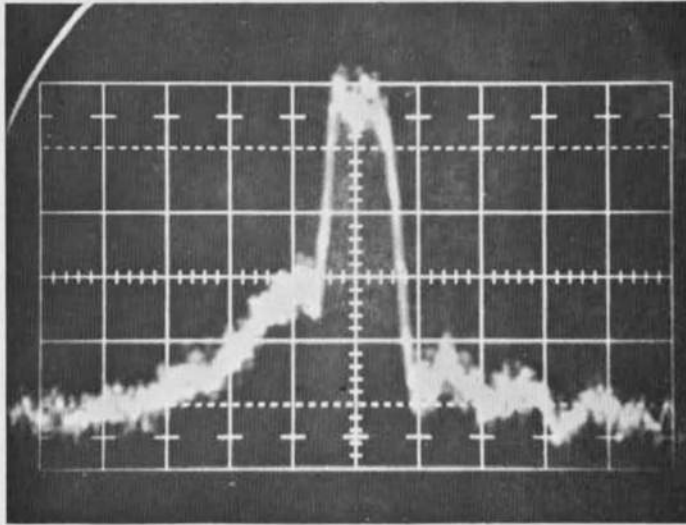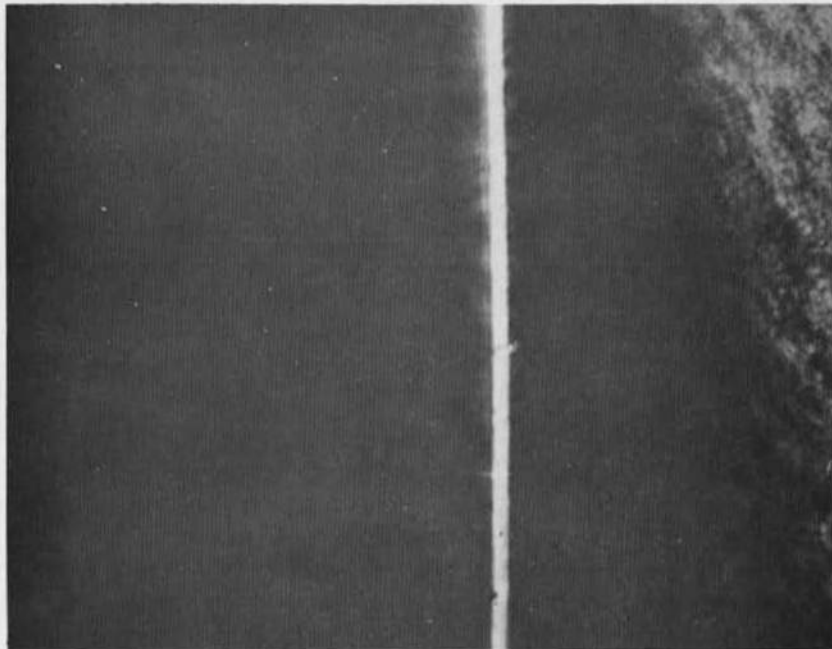
60

Figure 25. The plot of $\frac{A}{\pi} \ln \left| x_i - \frac{\tau}{2} \,/\, x_i + \frac{\tau}{2} \right|$

y axis: 50 mv/cm   x axis: 0.1 μsec/cm

(a) A horizontal scan line of the image plane
    attenuated by a neutral density filter

(b) The image plane as viewed on the TV monitor

Figure 26. The Hilbert transform of the step function.

or

$$U_i(x_i) = \frac{1}{2}[s_o'(x_i) + j\hat{s}_o'(x_i)] \tag{66}$$

The image intensity is

$$I_i(x_i) = \frac{1}{4}[s_o'^2(x_i) + \hat{s}_o'^2(x_i)] \tag{67}$$

When viewing a portion of a horizontal scan line showing the edge of the step function, the first term of Equation (67) is not detected since it is a constant. Only the second term of Equation (67) is detected and it is shown in Figure 27(a). The maximum image intensity amplitude is 500 mv. The edge of the step function appears as an intensity pattern with a width of 169 microns. The maximum error in locating the edge is 84.5 microns.

VII. BANDPASS FILTERING OF THE STEP FUNCTION

The bandpass filter is composed of two filters, a high frequency pass filter and a low frequency pass filter. The high pass filter is a number 20 AWG wire placed through the origin of the frequency plane. The low pass filter is effected by the finite diameter of the lens. The bandpass filtering of the step function is performed in the frequency plane of lens L2. The diameter of the lenses is 7.6 cm. The equation for the amplitude of the bandpass
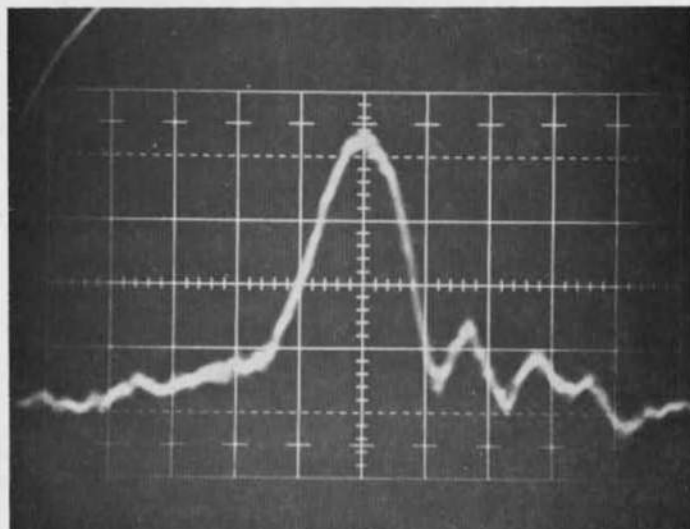
y axis: 100 mv/cm   x axis: 0.1 μsec/cm

(a) A horizontal scan line of the image plane
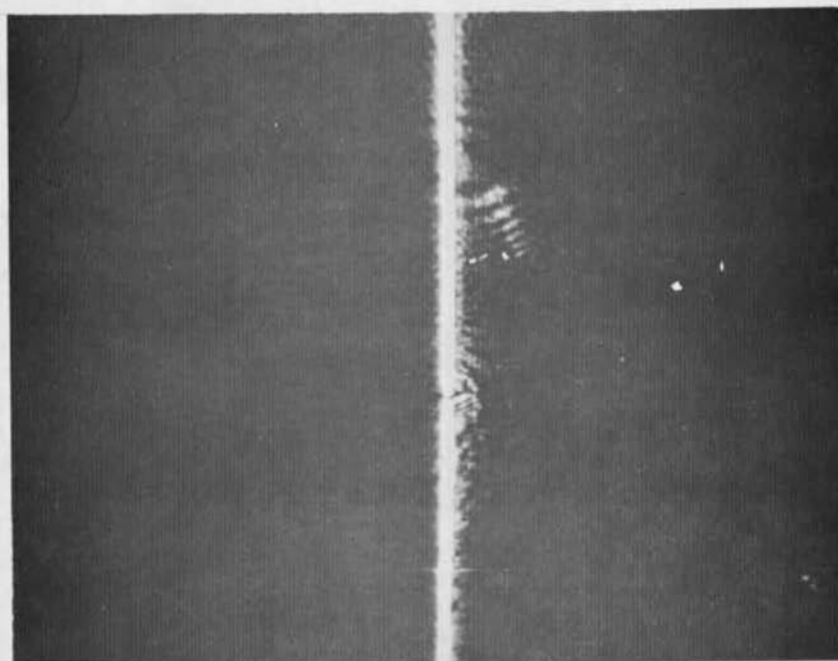
(b) The image plane as viewed on the TV monitor

Figure 27. The step function filtered by the Schlieren
   method.

filtered step function is derived by Fujimura [13]. The
equation is

$$G(x) = \frac{1}{\pi}[Si(2\pi bx) - Si(2\pi ax)] \tag{68}$$

For unity magnification where a is the lower spatial cutoff
frequency and b is the upper spatial cutoff frequency. G(x)
is the amplitude in the image plane and it is recognized as
an odd function. The amplitude of the positive half plane
is plotted in Figure 28 for different values of b. The
bandpass filtered step function appears visually as a
diffraction pattern which is symmetrical about the point
x = 0. The position of the horizontal scan line showing the
intensity of the bandpass filtered step function in the
image plane is shown in Figure 29. The "valley" in the
bandpass filtered step function occurs at x = 0. It is used
to locate the edge of the step function. The width of the
"valley" is 47.4 microns. The maximum error in locating the
edge is 23.7 microns. The signals' maximum intensity is
500 mv.

VIII. APPLICATIONS OF THE VARIOUS FILTERS

A summary of the operation of the previously con-
sidered filters upon a step function and the ability to
locate object edges is presented in Table I. The various
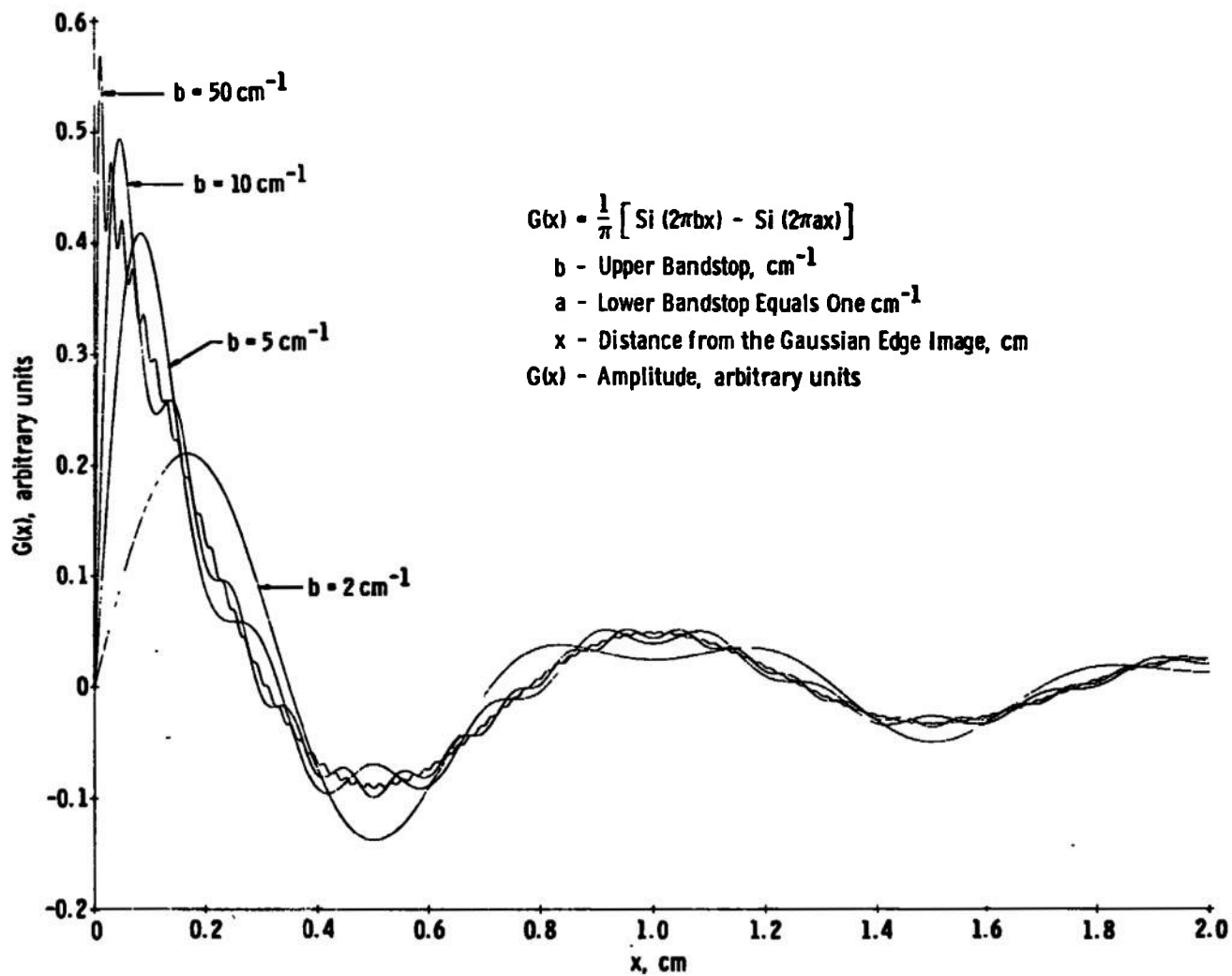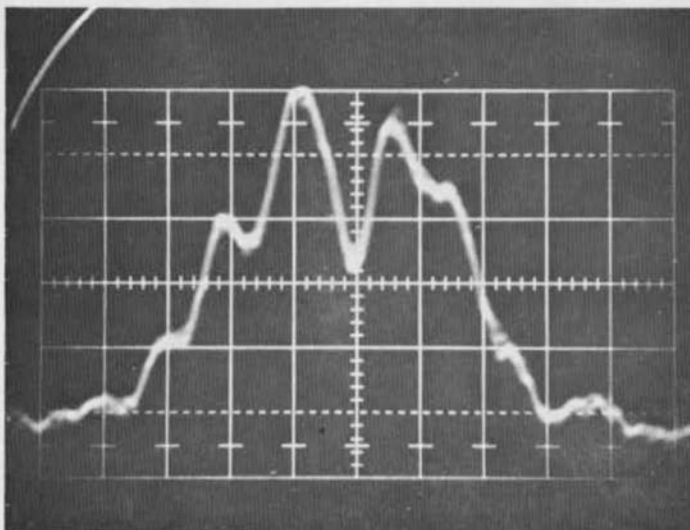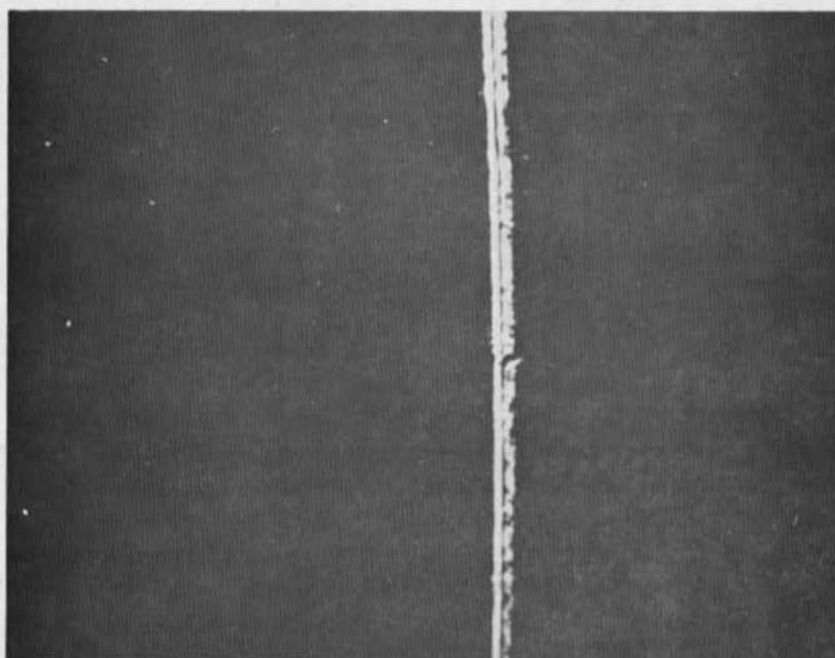optical filters were applied to different applications to

Figure 28.   Amplitude in a bandpass filtering image of
an Edge.

y axis: 100 mv/cm   x axis: 0.1 μsec/cm

(a) A horizontal scan line of the image plane

(b) The image plane as viewed on the TV monitor

Figure 29. Bandpass filtering of the step function.

TABLE I

SUMMARY OF THE EFFECTS OF VARIOUS FILTERS ON THE STEP FUNCTION

Step Function and Filter	Maximum Intensity of Signal in the Image Plane	Percentage of Attenuation	Maximum Error for Locating Edge
Unfiltered	4.28 volts	0%	
Differential Filter, $F'(\omega)$	0.13 volt	97.0%	54.00 microns
Linear Amplitude Filter, $A'(\omega)$	0.15 volt	96.5%	20.35 microns
Hilbert Transform	5.35 volts	−25.0%	169.00 microns
Schlieren Method	0.5 volt	88.3%	84.5 microns
Bandpass Filter	0.5 volt	88.3%	23.7 microns

provide an insight into their operation. The first example
is the wire mesh shown in Figure 30(a). The wire mesh is a
two-dimensional object. In Figure 30(b) the wire mesh is
filtered by the phase filter $\theta(\omega)$. The filter $\theta(\omega)$ is one-
dimensional. It yields the Hilbert transform of the wire
mesh only for the x-coordinate. The "smear" effect is
easily observed. Notice the y-coordinates are unaffected.
In Figure 30(c) the wire mesh is filtered by the approximate
one-dimensional filter $F'(\omega)$. Again, only the x-coordinates
are affected. The derivative is taken of both edges of the
vertical wires.

The second example is the hologram of an air
stream escaping at a high velocity from a nozzle into the
flow field of a wind tunnel. The disturbances in the center
of Figure 31(a) is the air stream from the nozzle. This
unfiltered air stream shows very little phase information.
In Figure 31(b) the flow field is filtered using the one-
dimensional Hilbert transform filter. The phase information
becomes very prominent, especially the air flow from the
nozzle. Notice the large shock wave which extends from the
top to the bottom of the figure. This shock wave is not
visible in Figure 31(a) since it is a small phase change.
In Figure 31(c) the flow field is filtered by the one-
dimensional Schlieren method. The large shock wave is
visible, but the phase information around the nozzle is not
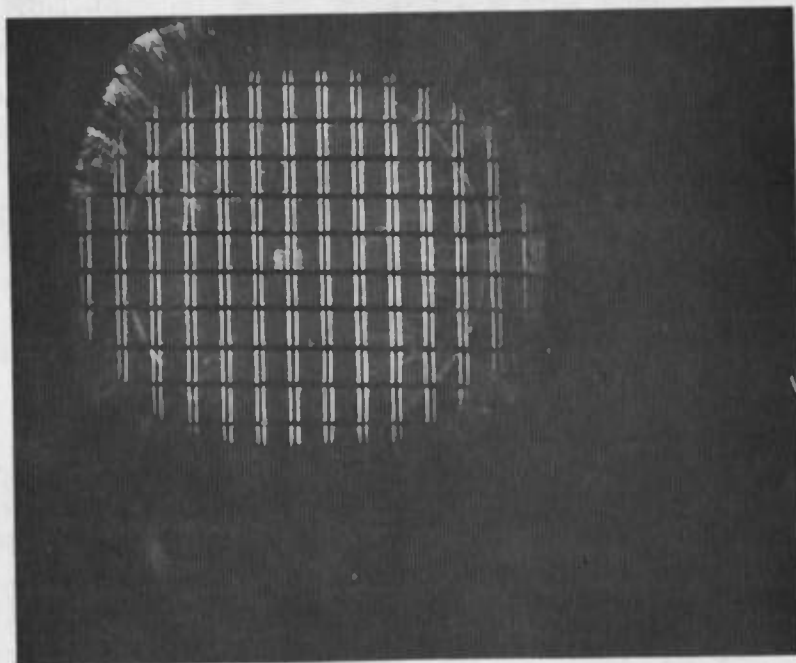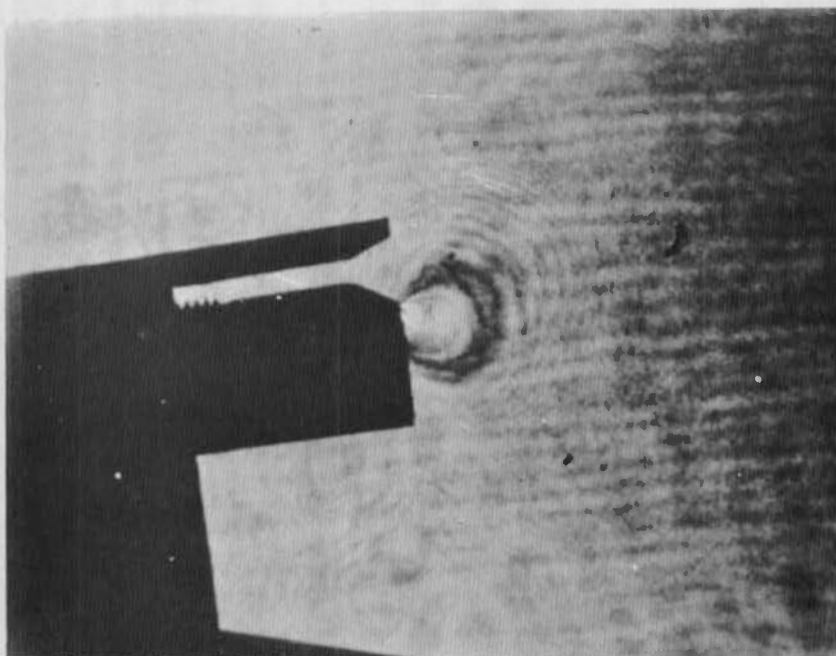visible. The phase information is affected by the

69
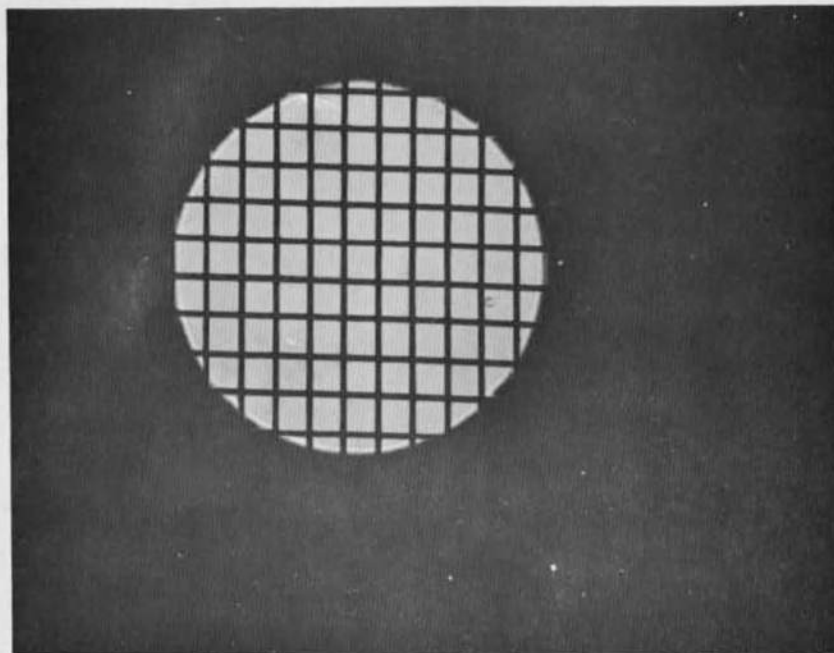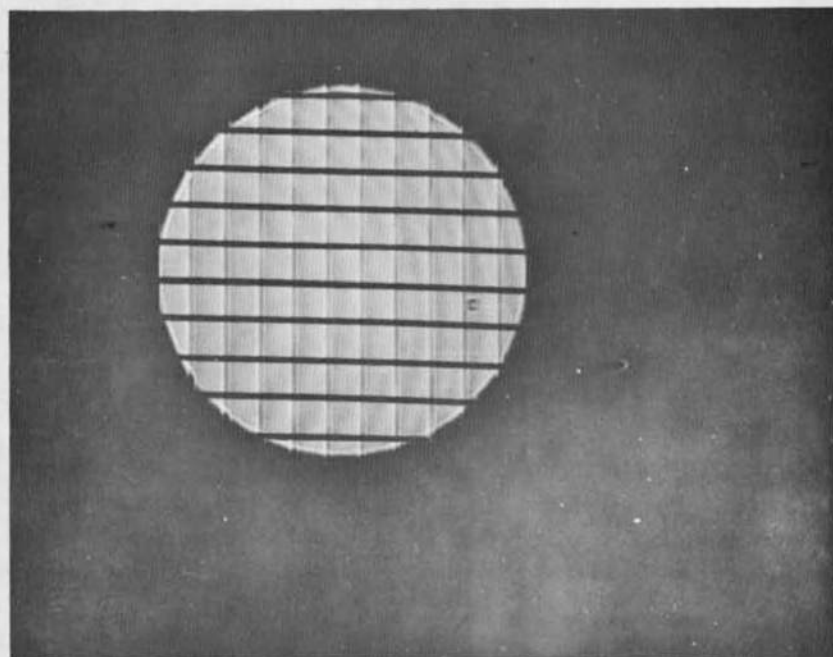
(a) Unfiltered

(b) Filtered by the filter $\theta(\omega)$
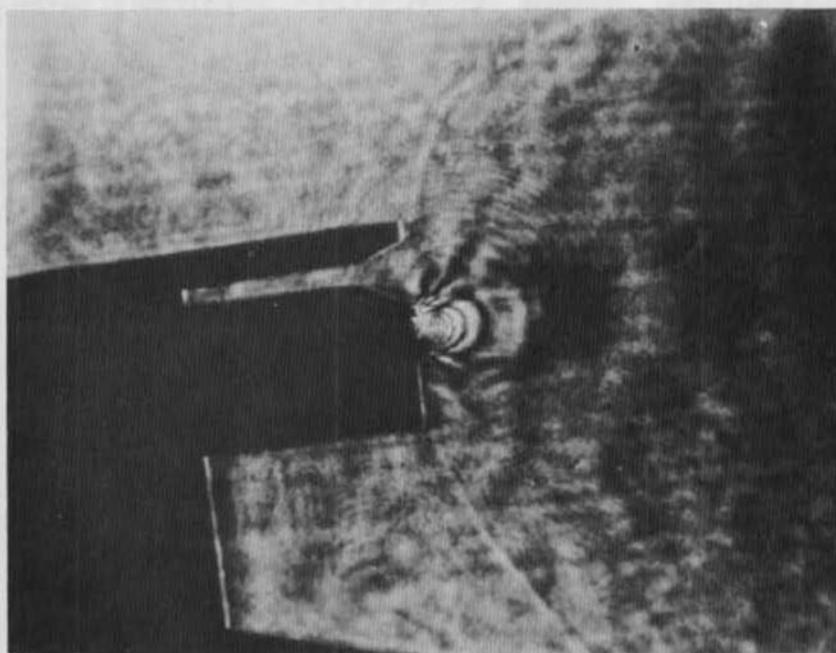
Figure 30. Filtering of a wire mesh.

(c) Filtered by the filter $F'(\omega)$

Figure 30. (continued)

(a) Unfiltered (flow is from left to right)

(b) Filtered by the filter $\theta(\omega)$

Figure 31.   Filtering of a flow field.

(c) Filtered by the Schlieren method

Figure 31.   (continued)

one-dimensional filter as long as it has an x-coordinate.
Filtering of the flow field by the differential filter $F'(\omega)$
was attempted, but the filter $F'(\omega)$ greatly attenuated the
information of the hologram, and no useful data were
obtained.

The third example is an air stream from a
compressed air gun striking the end of a rod. For the
unfiltered air stream, no phase information is visible.
When the air stream is filtered by the Hilbert transform
filter, the phase information becomes visible as shown in
Figure 32(b). The air stream is filtered by the differ-
ential filter $F'(\omega)$ in Figure 32(c). The differential
filter accentuates the phase information that is visible in
Figure 32(b). The one-dimensional differential filter
affects all information in the x direction.
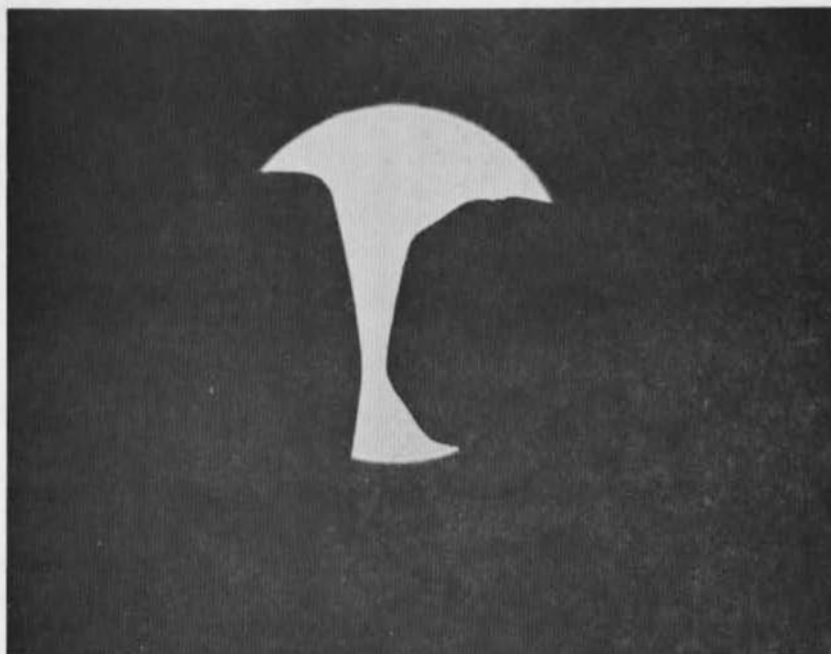
(a) Unfiltered (flow is from right to left)

(b) Filtered by the filter $\theta(\omega)$

Figure 32.   Filtering of a compressed air stream.

75

(c) Filtered by the filter $F'(\omega)$
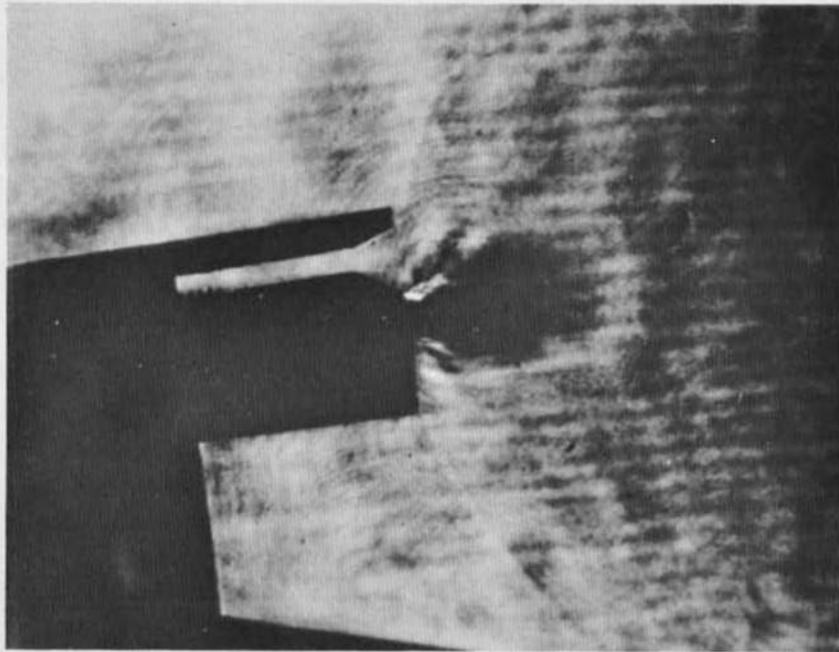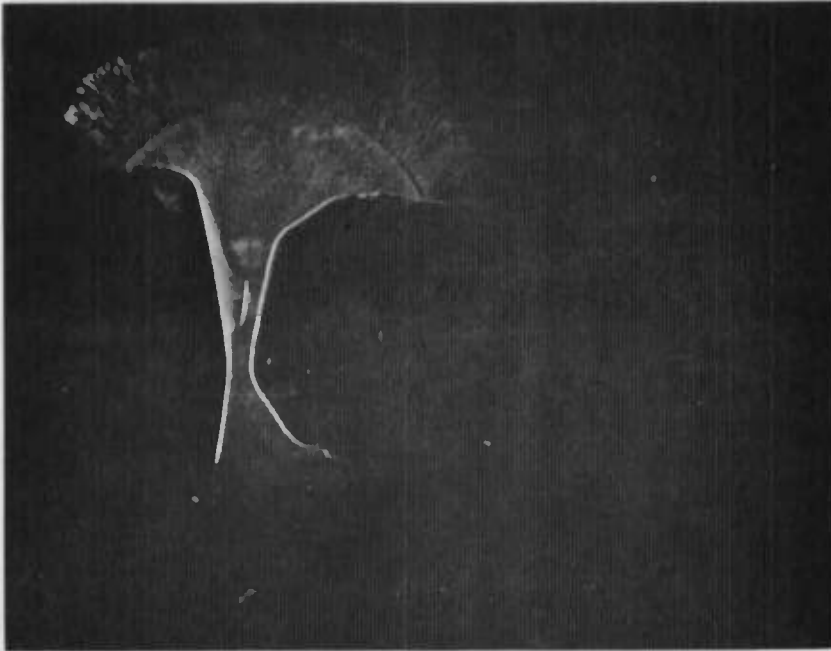
Figure 32. (continued)

CHAPTER IV

CONCLUSIONS

In this study a comparison was made between the differential filter, $F'(\omega)$, the linear amplitude filter, $A'(\omega)$, the Hilbert transform filter, $\theta(\omega)$, the Schlieren method, and bandpass filtering. Each filter was fabricated and tested. In addition, each of the various filters was applied to a step function to observe which filter was best for locating the edge of the step. Two conditions had to be taken into account when considering the various filters, the intensity of the filtered step function and the error in locating the edge.

It was found that the Hilbert transform method, or the phase filter $\theta(\omega)$, had too great an error in locating the edge, a 169 micron error. The Schlieren method had an error of 84.5 microns which was also too great when compared to the bandpass filter error of 23.7 microns. The linear amplitude filter, $A'(\omega)$, had the minimum error of 20.35 microns in locating the edge; however, its intensity was too low.

The intensity level of the step function filtered by the differential filter, $F'(\omega)$, was the lowest. However, the differential filter had an error of 54 microns in locating the edge which was twice as great as the error of

the bandpass filtering method and also of the linear ampli-
tude filter. Therefore, it was concluded that the bandpass
filter was the best filtering method for locating the edge
of the step function; in addition, except for the phase
filter, $\theta(\omega)$, it has the highest intensity level in
filtering the step function.

Next, the Hilbert transform filter, the Schlieren
filter, and the differential filter were compared in appli-
cations to test their ability to identify phase information.
The first application of the flow field in the wind tunnel
brought out the limitations of the differential filter since
it could not be used on a low intensity signal. When a more
intense signal was used, the differential filter produced
better results comparable to that of the Hilbert transform.
The Hilbert transform filtering of the flow field clearly
identified the phase information. When the flow field was
filtered by the Schlieren method, half the phase informa-
tion was obscured by noise, producing very poor results.
Thus, it appears in some cases that the best filter for
identifying phase information is the Hilbert transform
filter.

BIBLIOGRAPHY

BIBLIOGRAPHY

1. Goodman, J. W. Introduction to Fourier Optics. New
        York: McGraw-Hill Book Company, Inc., 1968

2. Carlson, A. B. Communication Systems: An Introduction
        to Signals and Noise in Electrical Communication.
        New York: McGraw-Hill Book Company, Inc., 1968.

3. Lowenthal, S., and Y. Belvaux. "Observation of Phase
        Objects by Optically Processed Hilbert Transform,"
        Applied Physics Letters, 11:49-51, July, 1967.

4. DeVelis, J. B. Theory and Application of Holography.
        Reading, Massachusetts: Addison-Wesley Publishing
        Company, 1967.

5. Eguchi, R. G., and F. P. Carlson. "Linear Vector
        Operations in Coherent Optical Data Processing
        Systems," Applied Optics, 9:687-694, March, 1970.

6. Lowenthal, S., and Y. Belvaux. "Recent Advances in
        Coherent Optics; Filtering of Spatial Frequencies;
        Holography," Revue d' Optique, Theorique et
        Instrumentale, 46:1-64, January, 1967.

7. Binns, R. A., A. Dickinson, and B. M. Watrasiewicz.
        "Methods of Increasing Discrimination in Optical
        Filtering," Applied Optics, 7:1047-1051, June,
        1968.

8. Lohmann, A. W., and D. P. Paris. "Computer Generated
        Spatial Filters for Coherent Optical Data
        Processing," Applied Optics, 7:651-655, April,
        1968.

9. Ichioka, Y., M. Izumi, and T. Suzuki. "Halftone
        Plotter and Its Application to Digital Optical
        Information Processing," Applied Optics, 8:2461-
        2471, December, 1969.

10. Friesem, A. A., and J. S. Zelenka. "Effects of Film
        Nonlinearities in Holography," Applied Optics,
        6:1755-1759, October, 1967.

11. Born, M., and E. Wolf. Principles of Optics. New York:
        Pergamon Press, 1965.

12. Wolf, E. Progress in Optics. Amsterdam: North
    Holland Publishing Company, 1969.

13. Fujimura, S. "Extraction of Characteristic Features
    from a Visual Pattern by Fraunhofer Diffraction,"
    Japanese Journal of Applied Physics, 7:60-69,
    January, 1968.

DOCUMENT CONTROL DATA - R & D

(Security classification of title, body of abstract and indexing annotation must be entered when the overall report is classified)

1. ORIGINATING ACTIVITY *(Corporate author)*	2a. REPORT SECURITY CLASSIFICATION
Arnold Engineering Development Center, ARO, Inc., Operating Contractor, Arnold Air Force Station, Tennessee 37389	Unclassified
	2b. GROUP N/A

3. REPORT TITLE

A COMPARISON OF VARIOUS COHERENT OPTICAL FILTERING OPERATIONS

4. DESCRIPTIVE NOTES *(Type of report and inclusive dates)*
Final Report

5. AUTHOR(S) *(First name, middle initial, last name)*

Robert Lee Cody, ARO, Inc.

6. REPORT DATE	7a. TOTAL NO. OF PAGES	7b. NO. OF REFS
June 1971	91	13

8a. CONTRACT OR GRANT NO. F40600-71-C-0002	9a. ORIGINATOR'S REPORT NUMBER(S)
Program Element 64719F	AEDC-TR-71-137
	9b. OTHER REPORT NO(S) *(Any other numbers that may be assigned this report)* ARO-OMD-TR-71-93

10. DISTRIBUTION STATEMENT
Approved for public release; distribution unlimited.

11. SUPPLEMENTARY NOTES	12. SPONSORING MILITARY ACTIVITY
Available in DDC	Arnold Engineering Development Center, Air Force Systems Command, Arnold AF Station, Tennessee 37389

13. ABSTRACT

A comparison is made of different coherent optical filters with respect to their ability to locate an edge and identify phase information. These different filtering methods are bandpass filtering, the Schlieren method, the Hilbert transform method, a linear amplitude filter, and a differential filter; these filters are one-dimensional. The differential filter is a combination of two filters, a linear amplitude filter and a Hilbert transform filter. A linear amplitude filter is made photographically by a programmed exposure of film to give the correct density variations. A Hilbert transform filter is a phase filter which is accomplished with a dielectric coating on glass. Bandpass filtering is accomplished by using a wire. With the use of a razor blade, the Schlieren method is achieved. The comparison of these filters indicated that bandpass filtering is superior for the location of an edge and that the Hilbert transform method is best for identifying phase information.

DD FORM 1 NOV 65 1473

14. KEY WORDS	LINK A		LINK B		LINK C	
	ROLE	WT	ROLE	WT	ROLE	WT
optical filtering						
bandpass filters						
dielectric filters						
photographic filters						
test facilities						

APK
Arnold AFS Tenn